Review article

Flexible polymeric patch based nanotherapeutics against non-cancer therapy

Houjuan Zhu [a], Justin Mah Jian Qiang [a,b], Chen Gang Wang [a], Chui Yu Chan [a], Qiang Zhu [a], Enyi Ye [a,c,**], Zibiao Li [a,c,***], Xian Jun Loh [a,*]

[a] Institute of Materials Research and Engineering, A*STAR (Agency for Science, Technology and Research), Singapore, 138634, Singapore
[b] Division of Chemistry and Biological Chemistry, School of Physical and Mathematical Sciences, Nanyang Technological University, Singapore, 637371, Singapore
[c] Institute of Sustainability for Chemicals, Energy and Environment (ISCE²), A*STAR (Agency for Science, Technology and Research), 1 Pesek Road, Jurong Island, Singapore, 627833, Singapore

ARTICLE INFO

ABSTRACT

Flexible polymeric patches find widespread applications in biomedicine because of their biological and tunable features including excellent patient compliance, superior biocompatibility and biodegradation, as well as high loading capability and permeability of drug. Such polymeric patches are classified into microneedles (MNs), hydrogel, microcapsule, microsphere and fiber depending on the formed morphology. The combination of nanomaterials with polymeric patches allows for improved advantages of increased curative efficacy and lowered systemic toxicity, promoting on-demand and regulated drug administration, thus providing the great potential to their clinic translation. In this review, the category of flexible polymeric patches that are utilized to integrate with nanomaterials is briefly presented and their advantages in bioapplications are further discussed. The applications of nanomaterials embedded polymeric patches in non-cancerous diseases were also systematically reviewed, including diabetes therapy, wound healing, dermatological disease therapy, bone regeneration, cardiac repair, hair repair, obesity therapy and some immune disease therapy. Alternatively, the limitations, latest challenges and future perspectives of such biomedical therapeutic devices are addressed.

1. Introduction

Nowadays, polymeric materials have been widely applied in biomedical fields and are favored in the development of tailor-made therapeutic devices owing to their biocompatibility, processability, and low cost [1–3]. Currently, soft materials based polymeric patches are extensively used as biomedical scaffolds for drug encapsulation or implantation due to their design flexibility and their ease to be endowed with stimuli-responsive features. In recent years, such polymers could be applied as several types of polymeric patches depended on the forming structure, such as microneedles (MNs), hydrogels, microcapsules, microspheres, and fibers. Such polymeric flexible matrixes are endowed with superior biocompatibility and biodegradability, avoiding an immunological response to a foreign substance and the easy patch

removal after surgery [4]. Besides for this, their hydrophilicity also could endow the hydrophobic therapeutic agents with long-term and internal stability during delivery process [4]. However, polymeric matrixes are most fabricated as the reservoir of nanoagents in diseases treatments.

Up to now, nanomaterials have been greatly employed as nanoagents for versatile nanomedical theranostics in light of inherent performances of different therapy modals [5,6]. Taking advantages of superior photothermal, electronic, optical, catalytic, magnetic, physical, and chemical features, these nanomaterials have been widely explored in various therapeutic modals, such as chemotherapy (CHT) [7,8], photothermal therapy (PTT) [9–11], photodynamic therapy (PDT) [12–15], chemodynamic therapy (CDT) [16–18], magnetothermal therapy [19,20], immunotherapy [21–23], radiotherapy (RT) [24,25], gene therapy [26,

27] and starvation therapy (ST) [28]. However, non-cancer treatment has a number of disadvantages when used alone, including long-term accumulation, high toxicity, instability and low bioavailability, limiting their future clinic application.

Through combining separate advantages of flexible polymeric patches and nanomaterials, nanomaterials embedded polymeric patches have received much attention of various therapeutic in bioapplication [26,29–32]. The integration of polymeric patches with various types of nanoparticles (NPs) [7,21,33,34], nanosheets [28,35–38], nanorods [27,39], metal organic frameworks (MOF) [40,41], micelles [42–44], and polymeric NPs [45] provided the capability to enhance the retention time of drugs, bioavailability, biodistribution, the efficiency and safety of drug delivery, stimuli responsiveness and multifunctional therapeutic demands, thus improving curative efficacy along with decreased systemic toxicity [46]. For instance, the drug-loaded nanomaterials facilitate the polymeric patches with high loading capability of drug and controllably on-demand drug release [47,48]. Because of these above unique merits, such nanomaterials integrated polymeric systems have been extensively applied for treating non-cancerous diseases, including diabetes therapy, wound healing, dermatological disease therapy, bone regeneration, cardiac repair, hair repair, obesity therapy and some immune disease therapy, realizing the more bioapplications in clinic.

Despite a plethora of systematic researches and studies regarding the development of tumor theranostics are gradually increasing in number, and design of polymeric materials as delivery devices in biomedicine has also been systematically summarized in a gradually rising number of reviews [6,49–51]. A detailed and comprehensive overview that introduces nanomaterial integrated polymeric flexible patches in non-cancerous therapy still does not currently exist. Here, we focus on introducing the latest development of nanomaterials integrated polymeric patches for treating non-cancerous diseases (Scheme 1). Such nanomaterials that are embedded in a variety of polymeric patches applied in non-cancer therapy are in detail compared and summarized in the recent literatures (Table 1). Based on the recently regarding research, these polymeric patches with a highlight on the synthetic strategies and materials were presented and divided into the following categories: MNs, hydrogel, microsphere, microcapsule and fiber. In the following, according to the types of non-cancerous treatment, we emphatically introduced these applications in diabetes, wound healing, dermatological disease, bone regeneration, cardiac repair, hair repair, obesity and some immune diseases. Besides, we also discussed the current problems of polymeric patches as the depots in the field of biomedicine. Lastly, we give a summary and an outlook on the challenges, opportunities and perspectives of nanomaterials incorporated polymeric patches in more biomedical fields.

2. Classification of flexible polymeric patches

Currently, flexible polymeric matrix has been extensively studied in the field because of some unique outcomes, such as excellent biocompatibility, high drug loading capability, low bio-toxicity and, as well as a simple and economical production procedure. A diversity of polymers with varying performance were utilized to manufacture different flexible matrixes to achieve suitable and superior polymeric treatment modality under the relevant environment. Based on the applied morphological structure, these polymeric matrixes can be categorized into three forms: MNs patch, hydrogel patch and microsphere/microcapsules. Anything but this their ability of protecting the incorporated nanomaterials or drugs from biological and physical disruption and releasing them by dissolving, swelling or degrading, other advantages and disadvantages were compared and shown in Table 2.

2.1. Microneedle arrays

Microneedle (MN) arrays are needles of 25 μm–2000 μm supported on a base or patch [52], it was first conceptualized as a non-invasive parenteral (transdermal) drug delivery system in 1971 with the first successful instance in 1998 using silicon MNs to deliver calcein [53,54].
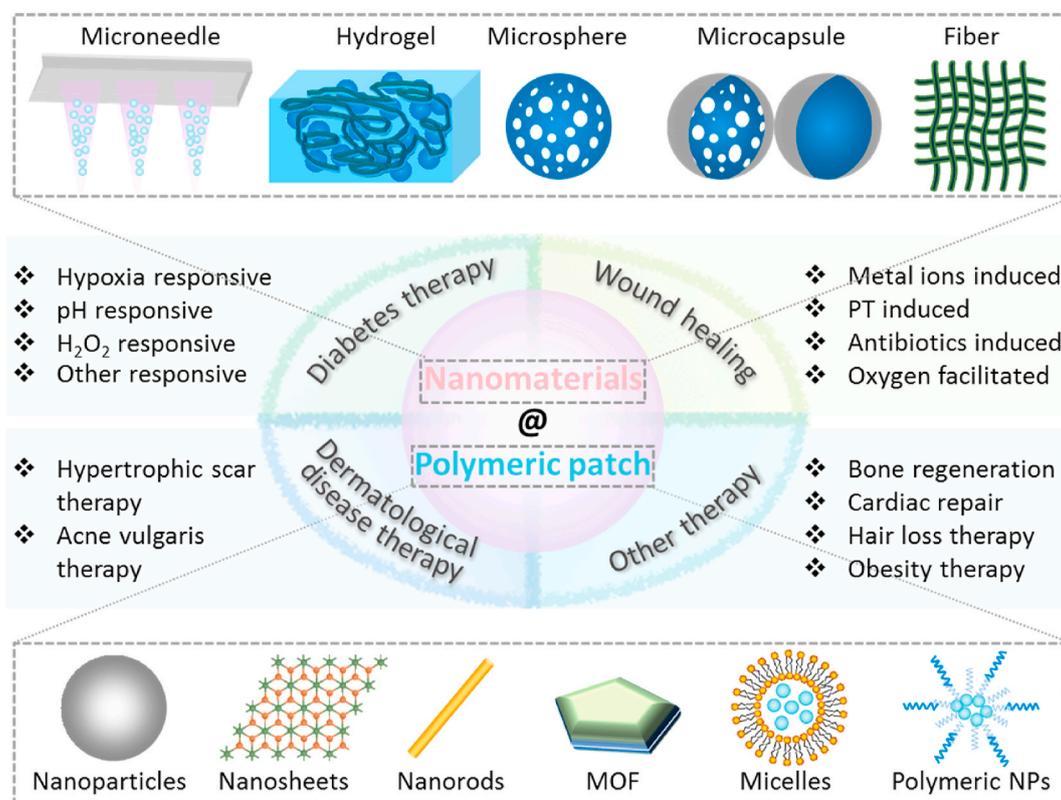
Scheme 1. Nanomaterials integrated polymeric patches for noncancerous disease treatment.

Table 1
Non-cancer therapeutics of nanomaterials integrated flexible polymeric patches.

Type	Characteristics of patch	Nanomaterials	Application	Property of treatment	Analytes	Ref.
MN	Dissolvability; biocompatibility	Black phosphorus	Wound healing	Oxygen Responsive	3T3 cells; STZ-induced diabetic mice	37
MN	Excellent biocompatibility; sufficient stiffness	H_2O_2-responsive polymeric vesicles (PVs)	Diabetes therapy	H_2O_2-responsive	HeLa cells; STZ-Induced diabetic mice	75
MN	High mechanical strength; biodegradation and long-term biocompatibility	MSC-derived exosomes; UK5099-loaded PLGA nanoparticles	Hair regrowth	Sustained drug release capacity	human dermal fibroblast cells, C57BL/6J mouse	77
MN	Improved the stiffness	Glucose responsive vesicles (GRVs)	Diabetes therapy	Glucose-responsive; hypoxia-sensitive; rapid responsiveness	STZ-induced diabetic mice	137
MNs	Biocompatibility; biodegradability	Self-assembled polymeric nanosized vesicles	Diabetes therapy	Hypoxia-sensitive	Mouse islets β-cells; STZ-induced type-1 diabetic SD mice	138
MN	Enhanced loading capability; bioavailability	Dual-sensitive, glucose-responsive polymersomes (d-GRPs)	Diabetes therapy	Hypoxia and H_2O_2 dual-sensitive	STZ-induced type 1 diabetic C57BL/6J mice	139
MN	Fast responsiveness; rapid hypoglycemic effect; no risk of hypoglycemia	Supramolecular polymer vesicles (PVs)	Diabetes therapy	pH- and glucose -responsive	3T3 cells; diabetic SD rats	141
MN	Improved mechanical strength	GO_x immobilized copper phosphate mineralized particles (m-GO_x); Ex4 integrated calcium phosphate (m-Ex4)	Diabetes therapy	pH- and, glucose-responsive; closed-loop release	C57BL/6 db/db diabetic mice	142
MN	Improved mechanical strength	ZnO quantum dots (ZnO QDs) capped mesoporous bioactive glasses (MBGs)	Diabetes therapy	pH- and glucose-triggered and	3T3-L1 cells; diabetes SD rats	143
MN	Remarkable mechanical strength; slower solubility properties; high strength; slow-release performance; Strong mechanical strength; excellent swelling property	$CaCO_3$ microparticles (INSCaCO_3 MPs)	Diabetes therapy	Swelling-responsive	MCF-7 cells; STZ induced diabetic rats	144
MN	Biocompatibility; improved robustness	HRP-CaP particles	Diabetes sensing	pH- and glucose-responsive; hyperglycemia sensing	STZ-induced diabetic mice	145
MN	Fast response; excellent biocompatibility; dissolvable	Polymeric vesicles (PVs)	Diabetes therapy	Glucose- and H_2O_2-responsive	STZ-induced type 2 diabetic SD rats	146
MN	Excellent mechanical strength and toughness	Mesoporous silica nanoparticles (MSNs)	Diabetes therapy	H_2O_2-responsive	STZ-Induced diabetes SD rats	147
MN	Enhanced strength	Nano-sized complex micelles (NCs)	Diabetes therapy	H_2O_2 and pH cascade-responsive	STZ-induced type-1 diabetic SD mice	148
MN	Improved mechanical strength	Gold nanoclusters (GNCs)	Diabetes therapy	Glucose-responsive	STZ-induced type-1 diabetic SD mice	149
MN	High loading efficiency; minimal toxicity	Polymer-grafted hollow mesoporous silica nanoparticles (HMSNs-PAPBA)	Diabetes therapy	Glucose-responsive	3T3-L1 cells; STZ rats	150
MN	High biocompatibility and biodegradability; relatively low melting point; dissolving; low cost; high loading capacity	Prussian blue nanoparticles (PB NPs)	Diabetes therapy	NIR light triggered	Muscle cells; STZ induced type 2 diabetic SD rats	151
MN	Dissolvable; excellent flexibility and toughness	Cu_7S_4 nanoparticles	Diabetes therapy	NIR light-triggered	HeLa cells; STZ induced type 2 diabetic SD rats	152
MN	Biodegradable; excellent flexibility and toughness; enhanced mechanical property	Hollow mesoporous SiO_2	Diabetes therapy	NIR-responsive	STZ induced type 2 diabetic SD rats	153
MN	Dissolvability	Proretinal nanoparticles (PRN)	Retinoids therapy	Sustained release	German domestic pigs	175
MN	Excellent aqueous solubility; rapidly dissolving; good biocompatibility	Bleomycin-loaded HA	Hypertrophic scar therapy	Rapid release	HHSFs cells	176
MN	Improved mechanical strength; improved loading of drug	HA/HP-β-CD complex	Hypertrophic scar therapy	Accelerated self-degradation	HSFbs cells, New Zealand rabbits	177
MN	Dissolvability	Mesoporous silica-coated upconversion nanoparticles (UCNPs@mSiO_2)	Abnormal scar therapy	Gene silencing	HSF cells	178
MN	Reactive oxygen species (ROS)-responsive; excellent biocompatibility and biodegradability	Diatomaceous earth (DE)	Acne vulgaris therapy	Controlled and sustained drug release	Infiltrated inflammation cells; P. acnes; P. acnes-induced mice	179
MN	Degradability; biocompatibility	Rosi-loaded NPs	Obesity therapy	Sustained release	C57BJ/6 mice	181
MN	Biocompatibility; rapid Dissolvability	DNA vaccine coated PLGA-PLL/Γpga NPs	Ebola vaccination	Supporting the safety and immunogenicity of the vaccine	HeLa cells	67
MN	Flexibility; dissolvability	DNA polyplex	Porcine circovirus Type 2	Stronger immune response; excellent vaccine stability	normal mouse	185
MN	Biocompatibility; dissolvability	DNA loaded RALA peptide NPs	Cervical cancer	Enhanced immune responses	C57BL/6 mice	186
MN		pOVA loaded nanopolyplex	Melanoma			187

Table 1 (*continued*)

Type	Characteristics of patch	Nanomaterials	Application	Property of treatment	Analytes	Ref.
	Dissolvability; sufficient mechanical strength			Stronger antigen-specific antibody response; enhanced antibody recall memory after challenge	DC 2.4 cells; RAW 264.7 cells; C57BL/6 mic	
Hydrogel	High intrinsic bioactivity; excellent mechanical strength,	Ultrathin 2D black phosphorus (BP) nanosheets; CaP crystal particles	Bone-tissue regeneration	Mimics biological mineralization	hBMSCs cells, MC3T3 cells	36
Hydrogel	Good biocompatibility	Gold-spiked silica microrods	Anti-bacteria	Plasmonic-induced photothermal anti-bacteria	E. coli	39
Hydrogel	Good biocompatibility; controllable porosity; degradability; swelling, rheological, mechanical, and conductive behaviors	Polydopamine-coated carbon nanotubes (CNT-PDA)	Wound healing	Photothermal anti-bacteria	L929 fibroblast cells; *S. aureus*, E. coli; Female Kunming mice	45
Hydrogel	Excellent biocompatibility and biological properties; improved mechanical properties	Ferritin nanocage	Tissue regeneration	pH stimulus; less cellular toxicity; good cellular growth, controllable and sustained drug release	NIH-3T3 cells	46
Hydrogel	Enhanced viability; mitigated hypoxia-induced cell death	Calcium peroxide (CPO)	Infarcted myocardial tissue regeneration	Controlled oxygen release	Photoinitiator (Irgacure 2959)	47
Hydrogel	Improved organization, electroactivity, mechanical integrity; improved cardiac cell adhesion, organization, and cell-cell coupling	Carbon nanotube (CNT)	Cardiac constructs	Promote electroactive tissue repair	MSCs cells	48
Hydrogel	Biocompatible paintable conductive, strong wet adhesive property	Polypyrrole (Ppy) nanoparticles	Cardiac tissue reconstruction	Faster self-degradation	L929 cells, BMSCs cells; SD rats	64
Hydrogel	Excellent operation ability; biocompatibility and most importantly	Stem cell-derived exosomes (SC-Exos)	Wound repair	Photoinduced imine crosslinking	New Zealand rabbits	88
Hydrogel	Biodegradability and biocompatibility; self-adhesive and conductive	Dopamine-functionalized polypyrrole (DA−PPy)	Infarcted myocardium construction	Biocleavable; mechanical supporting	L929 cells, H9C2 cardiomyocytes; SD rats	91
Hydrogel	Excellent antibacterial activity	Silver nanoparticles	Wound healing	Metal ion induced anti-bacteria	*S. aureus*, E.coli	155
Hydrogel	Relevant swelling capacity, good biocompatibility and mechanical properties	Silver nanoparticles	Wound healing	pH-Responsive; metal ion induced anti-bacteria	*P. aeruginosa*, S. epidermidis	157
Hydrogel	Excellent antibacterial properties; excellent injectability; biocompatibility	Zinc-doped bioactive glass (ZBG)/succinyl chitosan (SCS)/ oxidized alginate (OAL) composite hydrogels (Gel-ZBG)	Wound healing	Metal ion induced anti-bacteria	L929 cells; *S. aureus*, E. coli; SD rats	158
Hydrogel	High antibacterial efficiency	Ag/Ag@AgCl/ZnO hybrid nanostructures	Wound healing	Reversible swelling-shrinking transition by pH; metal ion induced anti-bacteria	MC3T3-E1 cells; *S. aureus*, E.coli; male Wistar rats	159
Hydrogel	Good mechanical stability; excellent tissue adhesion; self-healing properties	PF127 nano micelles	Wound healing	Antibiotic anti-bacteria	E. coli, *S. aureus*, 3T3 cells, B16F10 cells	160
Hydrogel	Stretchable compressible; self-healing injectable; pH-dependent biodegradation and release behavior,	PF127–CHO micelles (Cur-PF127-CHO)	Wound healing	Antibiotic anti-bacteria	E. coli, *S. aureus*; L929 cells; hemorrhaging liver mouse	161
Hydrogel	Excellent mechanical properties	Diacrylated Pluronic F127 micelles	Wound healing	Mechano-responsive; antibiotic anti-bacteria	S.epidermidis, E. coli; rabbit BMSCs	162
Hydrogel	Prevented multidrug resistance; minimized drug toxicity	Fe$_3$O$_4$@C nanoparticles	Wound healing	Visual and real-time monitoring of drug content; antibiotic anti-bacteria	L929 cells; *S. aureus*	163
Hydrogel	Inherent antimicrobia; antioxidant; cytocompatibility properties	silver Nanoparticles	Wound healing	Antibiotic anti-bacteria	S.aureus, P. acnes and Candida auris	164
Hydrogel	Superior antibacterial capacity; reduced inflammatory response; promoted angiogenesis ability	Cu nanoparticles (Cu NPs)	Wound healing	Photothermal anti-bacteria	NIH-3T3 cells; *S. aureus* and E.coli; SD rats	165
Hydrogel	Excellent and controlled photothermal ability	Oligomeric proanthocyanidins (OPC)	Wound Healing	Photothermal anti-bacteria l	B16F10 cells, nude Balb/c mouse; STZ diabetic C57BL/6 mouse	166
Hydrogel	Injectable photo–cross linked; biodegradability; biocompatibility; protection of loaded drugs	PLGA nanoparticles	Bone tissue repair	Sustained release	MSCs cells	167
Hydrogel	Improved strength and conductivity	Carbon nanotubes (CNTs)	Cardiac constructs	Improved cardiac cell functions	LX-2 cells; SD rats	169
Hydrogel	Injectable; sustainable; thermoresponsive	Copper sulfide nanodots	Obesity therapy	NIR-II photothermal-responsive	Primary human white preadipocytes; high-fat-diet fed mice	182
Fiber	Enhanced mechanical properties, wettability, thermal stability, biominerals deposition, and	2D MoS$_2$ nanosheets	Bone tissue regeneration	Thermal induced decomposition	MC3T3-E1 cells	38

Table 1 (*continued*)

Type	Characteristics of patch	Nanomaterials	Application	Property of treatment	Analytes	Ref.
Fiber	biocompatibility, proliferation and differentiation behavior Enhanced cell adhesion, growth, proliferation; enhanced bioactivity, biocompatibility and osteogenic differentiation	Polypyrrole nanoparticles (PPy–NPs)	Bone tissue regeneration	Electrical stimulation	MC3T3-E1 cells	118
Fiber	Strong biocompatibility, bactericidal, porous and mechanically	Silver nanoparticle	Wound healing	Metal ion induced anti-bacteria	NIH3T3 cells; *S. aureus*, E.coli	156
Microcapsule	Biocompatibility and biodegradability	PLGA microcapsules	Tissues regeneration	Mechano-activation	MSCs cells	115

Table 2
Comparison for advantages and disadvantages of different flexible polymeric patches.

Polymeric matrix	Advantages	Disadvantages
MN	Precise drug loading; High drug loading efficiency; Realizing instant transdermal drug delivery; Unique capability of swelling; Allowing attachment of drug reservoir; No measurable polymer residue leaving; Extracting the interstitial fluid from the skin and release of pre-loaded drugs; Easy remove after treatment; Treatment can be momentarily stopped; Proper biosafety and repeated use	Need more waiting-time to completely dissolve before removing the patch; Only used in epidermal disease treatment Limited drug loading into the polymeric matrix
Hydrogel	High drug loading efficiency; Unique capability of swelling; Usually employed for sustained drug release	Polymer residues found in skin within a few days; Influence of cross-linking conditions on bioactivity of drugs; Easy leaky of drug during delivery
Microsphere/ microcapsule	Increasing drug loading efficiency through encapsulation or coating;	Polymer residues found in skin within a few days; Slow self-degradation; Easy leaky of drug during delivery

Parenteral drug delivery methods such as MN arrays and injections offers several advantages over conventional oral drug delivery; namely the possibility of gastric irritation of some drugs [55], elimination of the drug through hepatic first-pass metabolism in the liver [56], and poor compliance of the patients [57]. Moreover, within parenteral drug delivery systems, MN arrays are preferred over injections as it does not cause bleeding, is pain-free, easy to apply, and does not generate non-ecofriendly biohazardous sharp waste [58].

MNs can be categorized into several types according to the mechanism of drug delivery [52], such as solid [59–61], hollow [61,62], coated [63–65], dissolving and hydrogel types. Usually, MNs are employed as a preprocessed stratagem, which could produce micro-channels to improve drug diffusion through inserting and withdrawing the MNs on the skin. Hollow MNs were reported to demand precision microfabrication techniques for constructing an interior lumen in each needle to inject drug, and commonly were used to facilitate drug delivery under the assistance an external driving force. The coated MNs were defined due to the loading of specific drug onto the surface of solid MNs to target delivery via dip coating, layer-by-layering coating, spray coating, and roll coating. These three MNs were most fabricated by inorganic materials including silicon and stainless steel by laser cutting and chemical etching, thus, this section will describe commonly used

polymeric MN materials and advances in recent MN based drug delivery systems.

2.1.1. Dissolving microneedles

Dissolving MNs are made of a bio-dissolvable material and generally holds the drug mixed in with the polymeric matrix, which eventually dissolves and releases the drug into the body. Such dissolving MNs are generally fabricated by pouring the polymer mixture and drug into a polydimethylsiloxane (PDMS) mold, and left to solidify, followed by a piece of adhesive on top of it as shown in Fig. 1A [66,67]. One of the most commonly used polymeric material for dissolving MNs is poly-vinylpyrrolidone (PVP) due to its biocompatibility and high dissolv-ability [68], which has been demonstrated to be capable of delivering all sorts of drugs [58,69,70], antibodies [71] and vaccines [66–68], both by itself and also in conjunction with other polymeric matrices. For example, Sung et al. reported the use of PVP MNs to deliver two model drugs, AlexaFluor-488 (Alexa-488) and subsequently Cyanine5 (Cy5) contained within pH-responsive hollow polymer microspheres. The MNs were successfully applied onto rat skin without breaking, and quickly dissolved within minutes to release the first drug (Alexa 488) and depositing into the tissues (Fig. 1B) [70]. The second drug (Cy5) encapsulated in hollow microspheres was subsequently released to neighboring tissues in an acidic environment. In 2020, it was demonstrated that the addition of magnesium (Mg) microparticles in dissolving PVP MNs allows a form of active delivery without external stimulus, as the H_2 gas generated act as "pumps" which enhanced the rate of delivery (Fig. 1C) [71]. By using the active delivery MNs, it was demonstrated to also be capable of delivering a macromolecule; cowpea mosaic virus (CPMV) nanoparticles for treatment of cutaneous melanoma, which was previously difficult to perform under passive delivery [66].

2.1.2. Hydrogel microneedles

Hydrogel MNs are made of polymeric materials that are capable of forming a three-dimensional (3D) cross-linked polymeric network, resulting in a porous structure that allows it to retain water. These properties allow hydrogel MNs to deliver hydrophilic drugs after absorption of interstitial skin fluid from a reservoir or within the hydrogel, in a controlled manner by variation of its pore size [72]. Several polymeric materials have seen uses as hydrogel MNs, such as polyvinyl alcohol (PVA) [73–75], poly(methyl vinyl ether-maleic acid) copolymer [74], and several other homopolymers and copolymers [76,77]. One of the drawbacks was that drugs compatible with hydrogel MNs were previously limited to those stable in aqueous environments. Recently, Donnelly's group demonstrated that the use of a non-aqueous directly-compressed tablets as a reservoir could facilitate the delivery of several drugs transdermally using hydrogel MNs including amoxicillin which hydrolyses in aqueous medium, greatly expanding the possibilities of compatible drugs [74].

2.2. Hydrogel patches

Hydrogel is a three-dimensional network of hydrophilic polymers, which can imbibe and retain water in its porous structure due to cross-
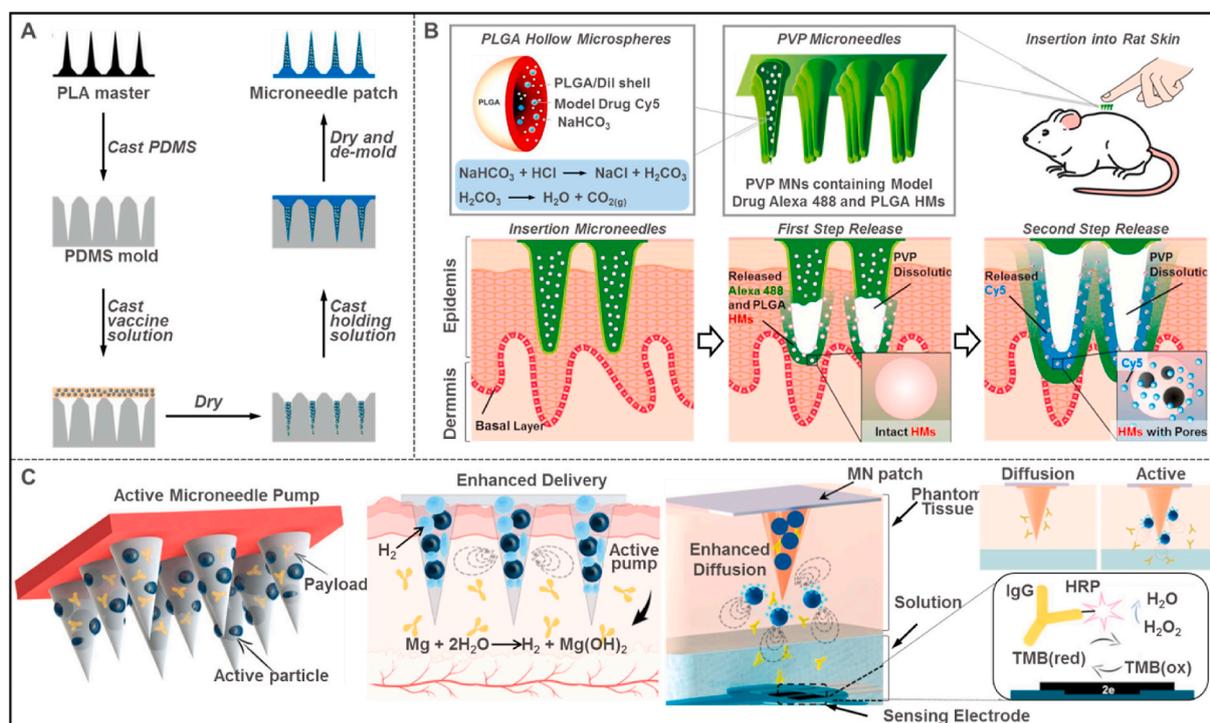
Fig. 1. A) Schematic Illustration of microneedles fabrication by PDMS cast molding. Reprinted with permission from Ref. [67]. Copyright 2017, Wiley. **B)** A schematic illustrating the design of the PVP MN arrays containing pH-responsive pH-responsive hollow microspheres (HMs) and the mechanism for delivering of two different drugs. PLGA: poly(*D,L*-lactic-co-glycolic acid). DiI: (1,1′-dioctadecyl-3,3,3′,3′-tetramethylindocarbocyanine perchlorate). Reprinted with permission from Ref. [70]. Copyright 2012, Elsevier. **C)** Illustration of the active delivery MN containing Mg particles, where contact with bodily fluids releases H_2 gas that act as "pumps". Reprinted with permission from Ref. [71]. Copyright 2019, Wiley.

linking of polymer chains [78–84]. The use of hydrogels in biomedical applications stems from its similarity to a tissue's extracellular matrix (ECM) [85], making it an attractive biocompatible polymeric material to hold hydrophilic drugs and other biomedical applications. One of the first few studies of the biomedical application of hydrogels was the potential of acrylate polymers for cornea surgical implants in 1965 [86]. Soon after, ethylene glycol methacrylate hydrogels was tested for subcutaneous application in rats in 1967 [87], followed by a study on its diffusion of anti-tumor drugs using methacrylate hydrogels in 1974 [88]. Since then, there have been many developments in this field with different kinds of natural and synthetic materials-based hydrogels, in which the common hydrogel materials used in various recent biomedical applications will be highlighted here. Up to now, hydrogel can be categorized into natural polymer based hydrogel and synthetic polymer based hydrogel depended on the applied polymer materials. Natural polymer based hydrogel was composited of nature polymers including alginate, hyaluronic acid, dextran, and chitosan, collagen, albumin, elastin, and gelatin [89–92]. These materials have all been developed for drug delivery applications due to their good tolerance in vivo, availability in abundance in nature, and ability to generate hydrogels via self-assembly or by cross-linking. The feature of spontaneously forming hydrogels for some natural polymers been used to construct smart delivery nanoplatforms that can be injected locally as a liquid and solidify into a hydrogel drug depot excited by the changes in the environment such as pH, temperature, or ionic composition. For this point, we will in detail introduce using gelatin-based hydrogels and hyaluronic acid-based hydrogels as examples in the following.

2.2.1. Gelatin-based hydrogels

Gelatin is a protein-based biomaterial which is obtained from hydrolysis of collagen, with good biocompatibility and biodegradability properties. However, it suffers from poor mechanical properties on its own without any cross-linkers. As such, gelatin is commonly used in conjunction with other compounds to optimize the mechanical features and offer additional properties [64,93–97].

One of such modification that is commonly used is gelatin methacryloyl (GelMA). GelMA was developed as a photo-crosslinkable hydrogel for creating microtissues, microfluidic devices and as a scaffold for epidermal tissue engineering. It demonstrated tunable mechanical, degradation and biological properties by variation of its methacrylation degree and hydrogel concentration [98,99]. GelMA has since been applied in all kinds of biomedical fields including drug delivery [46], cardiac patches [48], and tissue regeneration scaffolds [36, 100]. Khademhosseini and the co-wokers reported an oxygen-generating calcium peroxide (CPO) incorporated GelMA hydrogel as shown in Fig. 2A [47]. The biocompatible hydrogel was able to release oxygen and relieve the metabolic stress of cardiac cells under hypoxic conditions, significantly enhancing cell viability by reducing hypoxia-induced necrosis. Recently, Xu et al. demonstrated a biodegradable conductive hybrid hydrogel containing GelMA as the scaffold and polydopamine-modified black phosphorus (BP@PDA) nanosheets as the conductive component (Fig. 2B) [100]. The conductive GelMA-BP@PDA hydrogel was able to improve the mesenchymal stem cells migration into neural-like cells owing to the assistance of electrical stimulation, opening up the possibilities of materials used in electroactive tissue engineering.

2.2.2. Hyaluronic acid-based hydrogels

Hyaluronic acid (HA) is a polymeric glycosaminoglycan commonly found in body tissues and fluids. The abundance of HA in tissues, and possibility of chemical modifications due to the presence of easily modifiable functional groups [101], makes it an attractive material for a range of bioapplications such as drug delivery [41,102,103], cell culture and tissue engineering scaffolds [48,104] and more [97,105]. Cho and the coworkers incorporated either carbon nanotubes, polypyrrole, or both into catechol-functionalized HA hydrogels and fabricated
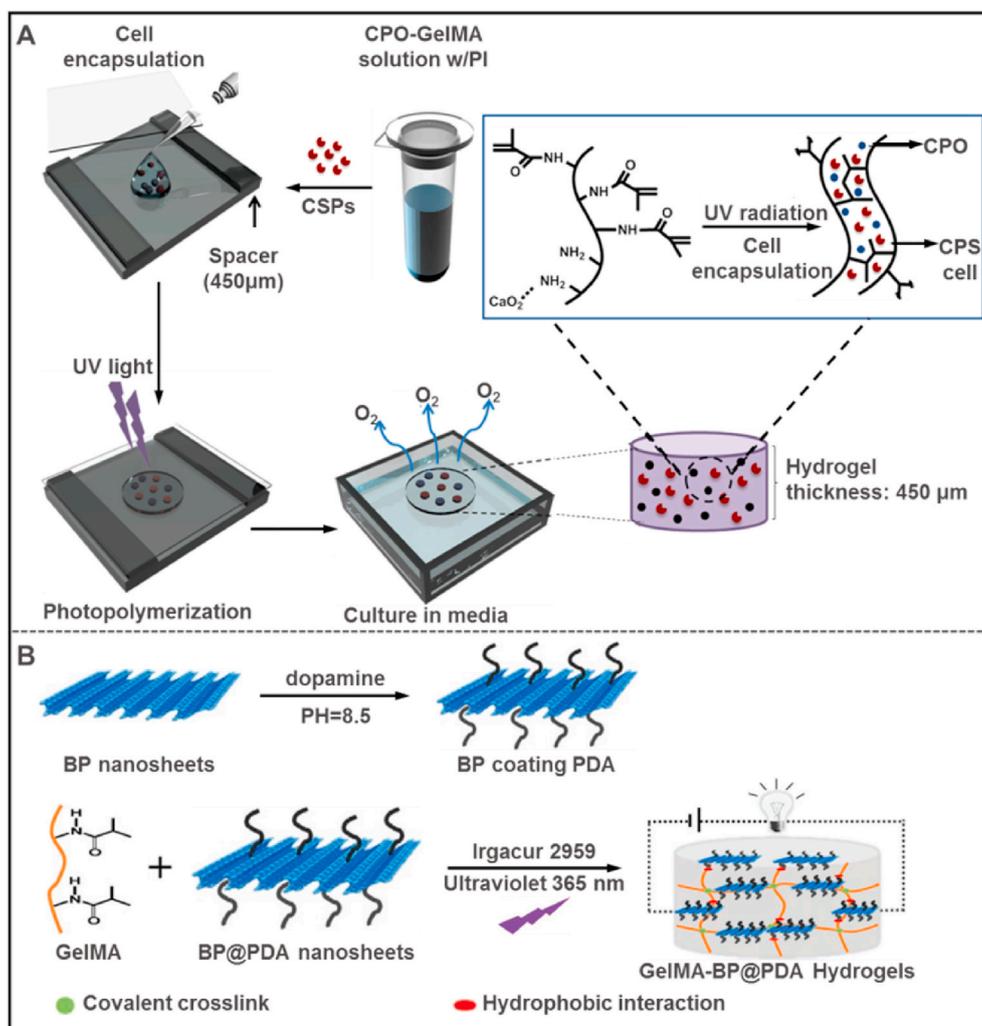
Fig. 2. A) Schematic illustration of the fabrication of GelMA hydrogels and the oxygen generation from encapsulated CPO. The GelMA hydrogels were prepared by mixing GelMA, CPO and cardiac side population cells (CSPs) *via* photopolymerization. Reprinted with permission from Ref. [47]. Copyright 2017, American Chemical Society. **B)** Illustration of the modification of black phosphorus (BP) nanosheets with polydopamine (PDA) and the incorporation of the BP@PDA nanosheets into GelMA hydrogel (GelMA-BP@PDA hydrogel). Reprinted with permission from Ref. [100]. Copyright 2020, Wiley.

electrically conductive hydrogels as a 3D ECM scaffold for cell culture and tissue engineering of stem-cell-mediated neuronal regeneration [104]. The same group reported that HA hydrogels modified with phenolic moieties exhibited stronger tissue adhesiveness and greater elastic modulus, which can then be transferred to an off-the-shelf form for clinical use which was previously difficult to achieve [106].

However, natural polymer exhibit some shortcomings [107]: 1) their poor solubility, especially in organic solvents, limits the processing possibilities and makes it more difficult to include water-insoluble chemotherapeutic drugs; 2) their biocompatibility necessitates great purity; 3) the lack of chemically tweaking polymer constitutions impacts critical features like drug release kinetics and degradation rate. Conversely, because synthetic polymers that used to prepare synthetic polymer based hydrogel, allow for such high levels of customization, local implants can be designed for specific applications in terms of mechanical qualities, degradation, and drug release. A large number of synthetic polymers including polyanhydrides based on sebacic and adipic acid, polyesters based on lactide, glycolide, caprolactone, and dioxanone, as well as polyamides polycarbonates, polyorthoesters, and phosphate-based polymers [108–110], have been used to fabricate various delivery materials. These polymers are frequently hydrophobic in nature, making them ideal for long-term delivery and internal stabilization of sensitive water-insoluble drugs. Although such synthetic materials have a disadvantage of forming acidic decomposed products, which can induce accumulation and inflammation at the implant site, this affection can be attenuated by modulation in chemical constitution and their degradation performance.

2.3. Other polymeric matrixes (microsphere/microcapsule/fiber/microchamber)

Apart from the well-studied microneedle and hydrogel matrixes, there have been other polymeric matrixes, such as microspheres, microcapsules, fibers and microchambers, which are capable or potentially capable of biomedical applications. In comparison with conventional drug administration methods, the use of polymeric matrices for drug encapsulation and releasing enable to prolong the active duration, minimize systemic toxicity, and protect the sensitive drugs from degradation.

Microspheres are spherical microparticles of diameters between 1 and 1000 μm, generally made of biodegradable polymers such as poly (lactic acid) and a copolymer of lactic acid and glycolic acid, with the drugs mixed in homogeneously [111]. The drugs were released after ingestion or injection of the microsphere. Microspheres have also been demonstrated to be compatible with microneedles [69,70] and hydrogels [112]. It was also capable of being a carrier for liquid metals for cancer chemophotothermal therapy [113]. Additionally, Liu et al. prepared poly(*D,L*-lactic-co-glycolic acid) (PLGA) microspheres containing doxorubicin (DOX) via electrospray [114]. The microspheres have a mean diameter of 6.74 ± 1.01 μm and were applicable for intratumoral injection. The *in-vitro* release test indicated that 12.3% and 85.8% of DOX released on day 1 and after 30 days, respectively. A higher local drug concentration at the target lobe of the liver was also detected, indicating that the microspheres are potentially useable as a drug delivery vehicle to targeted lesions.

Furthermore, microcapsules are spherical microparticles similar to microspheres, but instead of the drug mixed homogeneously, the drugs are encapsulated by a polymeric coating [115]. The release of drugs can be tailored to be in response to certain stimulus such as pH [116,117], temperature [117,118], light [119], magnetic field strength [120] and even mechanical input [121].

Also, up to today, fibers made from polymeric material have extensive uses in biomedical applications as scaffolds due to its similarity to ECM, desirable mechanical properties and possibilities for modification [122]. Fiber-like polymeric matrices have been uses in myocardial remodeling [123] and more commonly in tissue engineering and regeneration of bones [38,124–126], skin [127], and vascular system [128].

Beyond these patches, microchamber arrays, as one of most common polymer patches, contain individual micro-scaled voids on a flat polymeric matrix, and they are fabricated by microfabrication techniques such as multistep lithography or layer-by-layer assembly processes [129, 130]. Microchamber arrays are advantageous on their simple and low-cost processes using a universal mold and under arbitrary conditions. Similar with the other polymeric matrices, microchamber arrays can combine the stimuli-responsive functionalities, e.g., pH, light, temperature, or ultrasound, to control their shell permeability and drug releasing rate for site-specific release-on-demand [131–134].

3. Non-cancer therapy of nanomaterials incorporated polymeric patches

With the rapid development of global socioeconomics, a growing number of diseases have been found to become a global threat to human health, leading to the influence of human life. In addition to cancer that most is related to its occurrence and metastases [135,136], other noncancerous diseases, including diabetes [137], infected wound [138], cartilage damage [139], cardiac decease [140], obesity [141] and dermatological disease [142], have also dramatically increased and become the most serious public health problems in the 21st century. Within this context, it is an urgent requirement to explore effective treatments for these non-cancerous diseases. Currently, various treatments like surgery, CHT, RT, PTT, PDT, CDT, immunotherapy, have been developed as the main methods. Besides this, appropriate therapeutic nanoagents are highly desirable to been designed for enhanced efficiency and inhibition of diseases.

3.1. Diabetes therapy

Diabetes mellitus is a well-known chronic metabolic disease, which mainly depended on the failed blood glucose levels (BGLs) regulation. Generally, the traditional approach of curing patients suffered from type 1 and type 2 diabetes is to control normoglycemia level through applying insulin pumps or injecting insulin along with monitoring of glycemic levels. Such self-treatment with pain and nconvenience is usually not feasible to control glucose, increasing the biofouling risk in body. To avoid the aforementioned problems, a wide range of glucose-responsive insulin-releasing nanosystems have been developed to allow controllably insulin release for mimicking the β-cells. In view of the enzymatic reaction: $Glucose + O_2 + H_2O \xrightarrow{GO_x} Gluconic\ acid + H_2O_2$, glucose could be oxidized to generate H_2O_2 and gluconic acid under catalysis of glucose oxidase (GO_x) enzyme. Such GO_x-catalyzed reaction could be accelerated by consuming O_2, local hypoxia and decreasing pH in local microenvironment. In light of this, pH-, hypoxia-, H_2O_2- and other-responsive nanoplatforms have been extensively explored to construct controlled insulin delivery systems with fast response, high loading capability and superior biocompatibility though intercalating into flexible polymeric patch.

3.1.1. Hypoxia-responsive polymeric patch for diabetes treatment

By virtue of local hypoxia generation from O_2 consumption in the GO_x-catalyzed reaction, Gu et al. designed glucose responsive vesicles (GRVs) and incorporated a painless MN patch to establish a novel glucose-responsive insulin delivery device [143]. The insulin and GO_x enzyme co-loaded GRVs were responsive to hypoxia owing to self-assembly from hypoxia-sensitive 2-nitroimidazole conjugated HA (NI-HA). With the enzymatic oxidation of glucose, hypoxic microenvironment was formed to induce the reduction of hydrophobic NI to hydrophilic 2-aminoimidazoles by bioreducing agents, leading to GRVs dissociation and insulin release. When applied in type 1 diabetes induced animal model, this smart insulin delivery system could effectively regulate the BGL. This work firstly introduced to control insulin release activated by hypoxia, and its rapid responsiveness exhibited the potential to prevent hyperglycemia and hypoglycemia in diabetes therapy. Based on this concept, this group also provided "glucose-signal amplifiers" (GSAs) embedded MNs system for glucose-responsive regulation of BGLs [144]. Accounting for the hydrophobic-to-hydrophilic conversion of NI under hypoxia condition, GSAs were self-assembled by NI-HA and simultaneously entrapped GO_x, α-amylase (AM) and glucoamylase (GA). This design of "amplifier" is the first time to amplify the physiological signal for effectively transporting signal and mimicking the secretion of insulin from the β-cells. Inspired by this work, hypoxia and H_2O_2 dual-sensitive polymersome based vesicles integrated MNs were designed to regulate the BGLs (Fig. 3) [145]. The amphiphilic polymer composed of PEG) and NI modified polyserine *via* a thioether moiety can encapsulate insulin and GO_x by self-assembly (Fig. 3A). On account of the similar mechanism for conversion of hydrophobic IN to hydrophilic under hypoxia and introducing thioether as H_2O_2 sensitive moiety, such smart insulin patch was proved to high effectively regulate the BGLs in the diabetic mice with minimal side effect in regard to inflammation (Fig. 3B). This report offers new direction to design the dual-sensitive nanosystems for high oxidative stress and hypoxia related therapy.

In the past decades, a large variety of pH-responsive amphiphilic polymers have been broadly investigated for controlled drug delivery in the therapeutic application. Recently, pH-responsive a composite enzyme layer (CEL) was designed to coat mesoporous bioactive glass nanoparticles (BGNs) loaded with insulin, and subsequently incorporated into polymeric MNs [146]. In this case, the as-formed CEL composited of GO_x, CAT and polyethyleneimine (PEI) was served as glucose-sensitive layer and 'gatekeeper' for avoid the insulin leakage from BGNs. The pH decrease caused by the catalytic reaction by GO_x/CAT destroyed the CEL structure, resulting in the insulin release, rendering the BGLs regulation. Alternatively, Cen et al. integrated pH and glucose-responsive supramolecular polymer vesicles (PVs) used as the depot of insulin and GO_x with transcutaneous MNs [147]. The enzymatic catalysis of GO_x led to the declined glucose level and the decreased local pH, triggering the disassociation of PVs, contributing to the fast release of loaded insulin.

In addition to pH-responsive organic micelle for diabetes treatment, pH sensitive inorganic nanomaterials have also been employed to integrate with polymeric patch for control BGLs in diabetes. In a simple paradigm, pH-responsive mineralized calcium phosphate NPs immobilized with Exendin-4 (Ex4) and copper phosphate NPs encapsulated win GO_x were both integrated with flexible polymeric MN patch [148]. Noted that the embedded mineralized particles enabled the improved mechanical strength of MNs for painless and non-invasive transdermal administration while skin penetration. Under acidic condition, the dual mineralized NPs could spontaneously dissolve to separately release GO_x for regulating BGLs and Ex4 for diabetes therapy. Such glucose-responsive and closed-loop release system significantly enhanced Ex4 therapeutic efficiency, providing the insight of developing an effective approach for BGLs regulation in type 2 diabetes (T2D) therapy. Furthermore, Jiang and colleagues incorporated and mesoporous bioactive glasses (MBGs) loaded with insulin/GO_x/CAT and
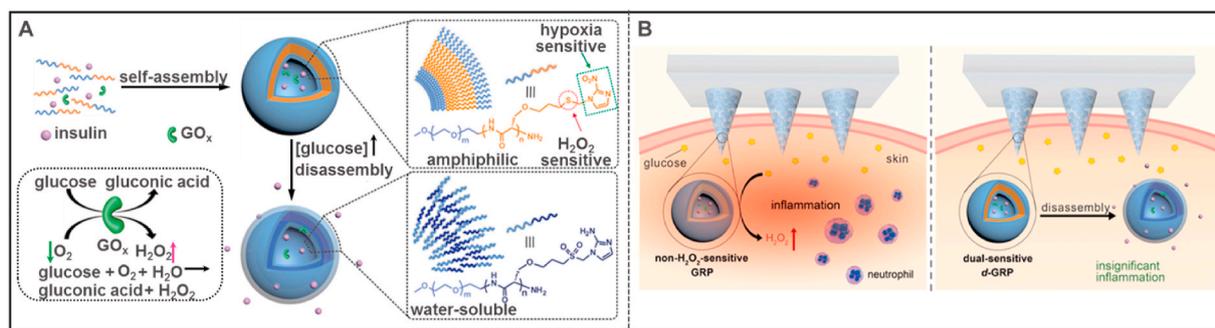
Fig. 3. Illustrative fabrication of hypoxia and H_2O_2 dual-sensitive polymersome-based vesicles (d-GRPs) loading MN patches, **A)** Mechanism of preparing d-GRPs coated by PEG-poly(Ser-S-NI); **B)** scheme for describing local inflammation induced by non–H_2O_2–sensitive GRP-loaded MN patch, and d-GRP-loaded MN patch for in vivo insulin delivery under a hyperglycemic state. Reprinted with permission from Ref. [145]. Copyright 2017, American Chemical Society.

capped with ZnO quantum dots (ZnO QDs) into polymeric MNs [149]. In the MBGs based MNs system, the nanopores of MBGs were sealed by insulin and GO_x/CAT, and subsequently caped by pH-sensitive ZnO QDs *via* electrostatic interaction. Under the low pH microenvironment, insulin and GO_x/CAT were gradually released by decomposition of ZnO QDs, allowing lower hypoglycemia risk. In another research work, insulin-loaded $CaCO_3$ microparticles (INS–$CaCO_3$ MPs) were integrated with polymeric MNs [150]. The low local pH led to the decomposition of

INS-$CaCO_3$ MPs, thus triggering the insulin release, allowing for glucose regulation. As another attractive paradigm, mimic multi-enzyme metal-organic framework (MOF) was deigned together with ethylene diamine tetraacetic acid (EDTA)-modified SiO_2 nanoparticles (EDTA-SiO_2 NPs) to embed into polymeric MNs (Fig. 4A) [40]. In this work, acid-sensitive MOF was engineered as the depots of insulin, GO_x and Co^{2+} to develop a catalase-mimic vehicle. Therein, GO_x in the MOF facilitated to reduce glucose, decrease local pH and generate H_2O_2.
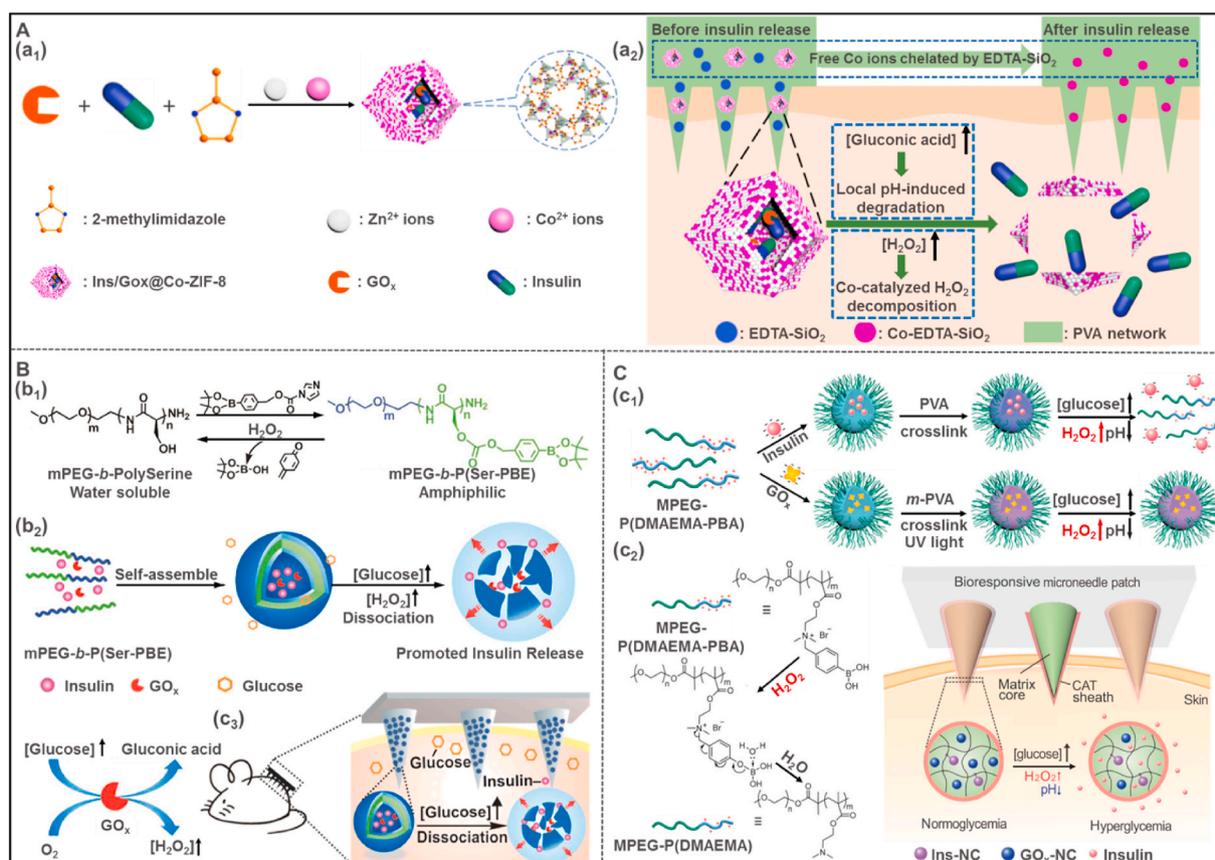

Fig. 4. **A)** Schematic description of synthesizing Mimic multi-enzyme ins/GO_x@Co-ZIF-8 and MOF-based MNs for glucose-mediated transdermal insulin release, **(a1)** Illustration of preparing multi-enzyme ins/GO_x@Co-ZIF-8, **(a2)** schematic depiction of MOF-based MNs for transdermal insulin release. Reprinted with permission from Ref. [40]. Copyright 2020, American Chemical Society. **B)** Schematic illustration of vesicles for glucose mediated insulin delivery, **(b1)** illustrative formation and degraded mechanism of mPEG-bP(Ser-PBE), **(b2)** schematic description of the self-assembly of PVs loaded with insulin and GO_x and their dissociation to release insulin under a hyperglycemic condition, **(b3)** illustrative diagram of PVs-based MNs patches for smart insulin delivery in a mouse model of type 1 diabetes. Reprinted with permission from Ref. [75]. Copyright 2017, American Chemical Society. **C)** Scheme of H_2O_2 and pH -responsive NC-loading MN-array patch for in vivo insulin delivery, **(c1)** illustrated description of preparing H_2O_2 and pH cascade-responsive NC-loading MN-array patch, **(c2)** schematic route for polymer synthesis, **(c3)** illustration of NC-containing MN-array patch for in vivo insulin delivery under a hyperglycemic state. Reprinted with permission from Ref. [154]. Copyright 2018, Wiley.

Under lower local pH, MOF could be decomposed to release insulin, and Co^{2+} from MOF could consume the generated H_2O_2, as well as extra Co^{2+} was chelated ETDA-SiO$_2$ NPs and eliminated along with MNs out. In short, such mimic multienzyme MOF-based MNs were proved to highly promising for diabetes treatment. Lately, pH responsive and HRP (horseradish peroxidase) caped calcium phosphate (CaP) NPs, 3,3',5,5'-tetramethylbenzidine (TMB) and GO$_x$ was combined to incorporate into MNs for colorimetric sensing BGLs [151]. On the basis of the GO$_x$-catalyzed reaction, the increased local acidity caused the CaP NPs decomposition, triggering HRP release. Such HRP could catalyze the reaction between the generated H_2O_2 and TMB, resulting in displaying color change at different BGLs.

As previous demonstrated, the generated H_2O_2 from GO$_x$-catalyzed reaction is elevated contributing to the concern of long-term biocompatibility and the problems of deactivating GO$_x$. With the aim of avoiding the negative effects and supplying O$_2$ for improving catalytic activity of GO$_x$, CAT and CAT related enzyme-mimicking nanomaterials have been employed in the diabetes treatment. Beyond that, the engineered H_2O_2-responsive nanoplatforms were reported to be as an alternative way for insulin delivery. In a typical example, Gu et al. created H_2O_2-responsive polymeric vesicles (PVs) integrated transcutaneous MN delivery device though cross-linked HA as the polymeric matrix [75]. The PVs was fabricated through self-assembly of polyserine (mPEG-*b*-P(SerPBE)) conjugated with phenylboronic ester (PBE) (Fig. 4B-b1), as well as loaded with insulin and GO$_x$. With the H_2O_2 generation via GO$_x$ catalyzed reaction, the PBE side chains was broken away from copolymer mPEG-*b*-P(Ser-PBE), resulting in dissociation of PVs, enabling the fast release of insulin (Fig. 4B-b1 and -b2). While applied in diabetic mice, the concentrated glucose under the hyperglycemic condition prompted PVs to release insulin with rapid responsiveness for regulating BGLs (Fig. 4B-b3). Once BGLs declined to normoglycemic state, the insulin release would gradually stop, thus circumventing hypoglycemia risk. In consideration of PBE as H_2O_2-sensitive block, Liu and co-worker synthesized a triblock copolymer including poly(ethylene glycol), poly(phenylboronic acid) as glucose-sensitive block, and poly(phenylboronic acid pinacol ester) as H_2O_2-sensitive blockas, which was self-assembled to form PVs [152]. The PVs loaded with insulin and GO$_x$ were integrated with polymeric MNs for transcutaneous delivery. Under hyperglycemic states, the basal insulin release enabled the elevated glucose, which would produce H_2O_2 through the catalytic function of GO$_x$. The generated H_2O_2 further led to destroy the chemical links of phenylboronic acid pinacol ester group, completely releasing insulin. Except this, H_2O_2-responsive PBE group was modified on the surface of mesoporous silica nanoparticles (MSNs) *via* a host-guest complexation with *a*-cyclodextrin (*a*-CD). Such MSNs were further encapsulated in to MN together with insulin and GO$_x$ to form a glucose-mediated MN delivery device [153]. Though the aforementioned mechanism, H_2O_2 originated from GO$_x$-catalytic reaction led to break the PBE link, destroying the disassembly on the surface the drug-loaded MSNs, finally triggering release of the preloaded insulin. Recently, a H_2O_2 and pH cascade-responsive nano-sized complex micelles (NCs) integrated MN system was constructed for transcutaneous insulin delivery by Gu's group (Fig. 4C) [154]. Such NCs were self-assembled from positively charged mPEG-P(DMAEMA-PBA) that was comprised of amphiphilic copolymer poly(ethylene glycol)-(2-(dimethylamino)ethyl methacrylate) (mPEG-P(DMAEMA)) and the modified 4-(bromomethyl) phenylboronic acid (PBA). GO$_x$ and insulin were successively entrapped into degradable NCs to form GO$_x$-NCSs and Ins-NCs, which were both further embedded into polymeric MNs together with catalase nanogel (CAT-NG). Under a hyperglycemic state, due to enzymatic functions of GO$_x$ and CAT, the low local pH and generated H_2O_2 caused trigger the rapid and safe release of insulin, thus enabling the effective control of BGLs.

3.1.2. Glucose/NIR light/ultrasound-responsive polymeric patch for diabetes treatment

In view of the related reports and the GO$_x$ catalytic reaction, glucose is the direct and major factor for self-regulation of BGLs in diabetic patients. Lei et al. designed glucose-responsive gold nanoclusters (GNCs) incorporated MN patch for responsive and transdermal insulin delivery [155]. With the modification of phenylboronic acid-derived molecules, GNCs as the nanocarriers possessed extremely high loading capacity of insulin. Under hyperglycemic condition, insulin was effectively and rapidly released from GNCs due to the stronger binding capability of glucose with diol units on phenylboronic acids than that of insulin. Lately, glucose-responsive poly(3-acrylamidophenylboronic acid) (PAPBA) was designed to decorate hollow mesoporous silica nanoparticles (HMSNs), which was integrated with MNs to form a transcutaneous delivery system [156]. At a typical hyperglycemic level, the grafted PAPBA polymer as gatekeeper of metformin loaded HMSNs was protonated to open the mesopores of the metformin release, achieving the effective BGLs regulation.

Apart from the issue that is related to GO$_x$ catalytic reaction, some unique strategies used in drug delivery system that are the remotely controllable release of drug have also been employed for diabetes management, such as NIR light, ultrasound. In a simple paradigm, Jiang and collogues incorporated prussian blue nanoparticles (PB NPs) and metformin into dissolving MNs patch using polycaprolactone (PCL) as polymeric matrix [157]. Under NIR light irradiation, PB NPs with photothermal effect produced heat, which could melt PCL polymer, thus enhancing the mobility of polymer chains, allowing for the metformin release. Similarly, they utilized Cu$_7$S$_4$ nanoparticles as the photothermal agents, metformin as the hypoglycemic drug and LA/PCL as the MN arrowheads to construct NIR responsive MN delivery system for controlling the BGLs [158]. In another design from same group, hollow mesoporous SiO$_2$ load with metformin was functionalized with polydopamine (PDA) as the photothermal agent and lauric-acid as the phase change material, which was further embedded into MN to form a NIR-responsive polymeric MN device [159]. When inserted into skin, the LA would melt on account of photothermal effect of PDA with NIR irradiation, leading to the metformin release. Besides those, insulin-loaded PLGA nanocapsules were embedded into chitosan microgels to construct an ultrasound-responsive delivery system [160]. With the ultrasound treatment, the microgels could rapidly respond to release insulin, effectively achieving BGLs control in a pulsatile, localized, and noninvasive manner.

3.2. Wound healing

It was acknowledged that the most common therapy technique of epidermal disease including melanoma, diabetes is surgical resection in the clinic, which was accompanying with the package on the wound with bandages, cotton wool, and gauze. While such method could make the large wound difficult to heal owing to the infection of diabetic wounds and the recurrence of cancer. In order to achieve the enhancement in the healing efficiency of infected wound, it emerged to be desirable for developing various dressings like flexible polymeric matrix with multifunctional characters and antibacterial capabilities to promote wound-healing. Recently, an increasing number of nanoplatforms with various therapeutic properties have been extensively expanded to optimize wound regeneration with high efficiency through combing with dressings.

3.2.1. Meal ion induced wound healing

Some common metal based nanoparticles were reported to release the corresponding metal ions for application in wound healing attributed to their excellent antibacterial activity and the ability of promoting fibroblasts generation. Therein, silver nanoparticles (Ag NPs) were extensively studied as antibacterial agents through producing physical damage to the cell membrane, generating ROS, and inflicting the

dysfunction of key components following by the release of Ag$^+$. For example, Ag NPs and Ag NP/clay/activated carbon biocomposites were synthesized by green chemistry approach to intercalate into PVA hydrogel patches (Ag NP-HP and Ag NP-Bc-HP) [161]. Such Ag NP-HP and Ag NP-Bc-HP exhibited good antibacterial activity with the minimum inhibitory concentration (MIC) of 25 μg/mL and 12.5 μg/mL for *Staphylococcus aureus* as well as 3.13 μg/mL and 6.3 μg/mL for *Escherichia coli*, respectively. The highly healing efficiency of wound was demonstrated through fixing such patches in wound incision on the dorsal skin of these rabbits, proving the hydrogel patches to be a promising candidate for wound healing. Similarly, Ag NPs was applied to functionalize with a porous polyacrylonitrile (PPAN) membrane under the assistance of mussel-inspired polydopamine (PDA) to form nanofiber patches [162]. Taking advantages of Ag NPs and PDA, hydrophilicity, mechanical properties and antibacterial activity of such patches were greatly improved and endowed, successfully realizing their wound-healing of such nanofibers. Additionally, a sensitive pH-responsive hydrogel patches integrated with Ag NPs were built for controlled and pH-triggered release [163]. Particularly, with the change of pH from acidic to alkaline, Ag$^+$ from Ag NPs was substantially increased. *In vitro* antibacterial studies of this hydrogel patch showed effective elimination of bacteria, indicating its potential as a novel nanoplatform to heal infected wound. Except for Ag NPs, ZnO nanoparticles (ZnO NPs) were also applied for wound healing to improve the generation of fibroblasts, thus inducing the proliferation and differentiation into myofibroblasts in wound. In a simple but creative paradigm, Hong et al. recently designed zinc-doped bioactive glass (ZBG)/succinyl chitosan (SCS)/oxidized alginate (OAL) composite based hydrogels (Gel-ZBG) for improved wound repair [164]. Within this hydrogel patch,

Schiff-based linkages were introduced for proliferation of cells in wound location, Zn^{2+} released from ZBG and amino groups from SCS endowed the composite hydrogels with superior antibacterial features, simultaneously Si^{4+} and Ca^{2+} released from hydrogels also could stimulate fibroblasts for angiogenesis and wound closure. Further, epidermal growth factor (EGF) was chosen to load into hydrogel for enhancing tissue remodeling and cell proliferation in the wound bed. All in all, such design provided a promising nanoplatform for wound healing. For a more effective paradigm, in combination of advantages of Ag$^+$ and Zn^{2+} in wound healing, Wang et al. fabricated Ag/Ag@AgCl/ZnO hybrid nanostructures to embed into a hydrogel to form the nanoparticles integrated hydrogel patch for improving wound healing and mitigating bacterial infection using a simple two-step technique (Fig. 5A) [165]. In particular, the Ag/Ag@AgCl nanostructures were firstly synthesized by assembling in the hydrogel though an ultraviolet light chemical reduction and ZnO nanostructures were subsequently embedded into the hydrogel via NaOH precipitation. Within the hydrogel patches, The Ag/Ag@AgCl nanostructures could produce the increased ROS via activation of the visible light irradiation, leading to the significant enhancement of antibacterial and photocatalytic activity from ZnO. Due to the great photogeneration of ROS, such hydrogel patch with a rapid sterilization could induce the mortality rate of 95.95% for *E. coli* and 98.49% for *S. aureus*, thus facilitating the wound healing. Besides, this hydrogel system could afford to controllably and sustainably release Ag$^+$ and Zn^{2+} through the reversible swelling-shrinking transition of hydrogel stimulated the pH change in biological microenvironment. Such release of Ag$^+$ and Zn^{2+} was responsive to the immune function to generate a plenty of white blood cells and neutrophils that were 2–4 times compared with that of the control, thus resulting in synergistically
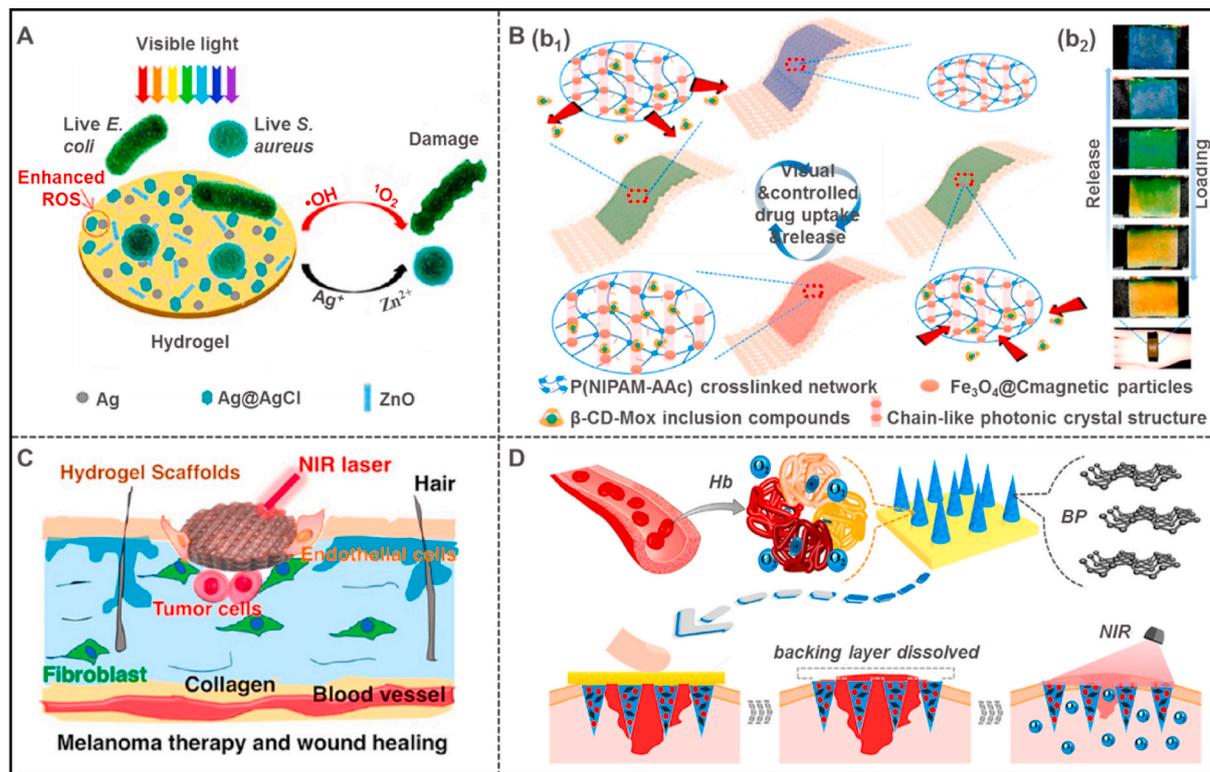

Fig. 5. A) Illustrative description of Ag/Ag@AgCl/ZnO hybrid nanostructures embedded hydrogel and the mechanism for wound healing by photo-inspired antibacterial. Reprinted with permission from Ref. [165]. Copyright 2017, American Chemical Society. **B)** Schematic illustration of hydrogel-functionalized textiles for optical screen of drug release and wound healing, **(b1)** preparation process of thermochromic hydrogel-functionalized textiles and the principle of drug release, **(b2)** optical photos of hydrogel-functionalized textiles with antibiotic loading or release. Reprinted with permission from Ref. [169]. Copyright 2019, American Chemical Society. **C)** Schematics of OPC-embedded hydrogel scaffolds for wound healing and melanoma therapy. Reprinted with permission from Ref. [172]. Copyright 2020, American Chemical Society. **D)** Scheme of NIR responsive separable MNs encapsulated with BP QDs and oxygen carrying Hb for wound healing. Reprinted with permission from Ref. [37]. Copyright 2020, American Chemical Society.

inhibiting bacteria and accelerating wound healing.

3.2.2. Antibiotic induced wound healing

Besides these, modern medicine that is dependent on antimicrobial agents including antibiotics is also reported to be an alternative strategy to prevent wound infection through destroying pathogens or inhibiting their growth. Controllable site specific delivery of antimicrobial agents provided the enhanced efficiency of wound healing accompanying with fewer side effects by increasing target site concentration. Lately, an increasing number of antimicrobial loaded wound dressings have developed for effective wound-management. Especially, a series of F127 based self-healing injectable micelle/hydrogel composites were designed as dressing for wound healing through loading a wide range of antibiotic drug including curcumin and paclitaxel (PTX) [166–168]. Such hydrogel patches with self-healing and excellent mechanical property could be biodegradable to controllably release these drugs triggered by pH and mechanics, thus offering the potential as a dressing for improving joints skin wound healing. In addition, it has received much popularity to introduce on-demand released systems for real-time monitoring of drug dosage and effectively healing on wound with enhancing treatment efficiency and reduced inverse affect. For an alternative typical paradigm, One-dimensional, chainlike photonic crystal structure (1D PCs) based on Fe_3O_4@C nanoparticles were fabricated to intercalate into poly(N-isopropylacrylamide-co-acrylic acid) (P (NIPAM-AAc)) hydrogel-functionalized textiles to form a novel wound patch (Fig. 5 B-b1) [169]. Such wound patch exhibited on-demand drug release accompanying with visual real-time identifying of drug content. Particularly, with the increased content of hydrophilic comonomer acrylic acid (AAc) introducing to store the drug, the lower critical solution temperature (LCST) of PNIAPM was adjusted to 40 °C, realizing the mild thermal stimulated and on-demand drug release. Fe_3O_4@C nanoparticles were embedded into PCs with the assistance of uniform magnetic field, causing the lattice spacing of PCs. Therein, on account of the variation of the lattice spacing (d) in PCs with the contraction and expansion of hydrogels, the color of such hydrogel-functionalized textiles made a difference, displaying the content of drug uptake or release from hydrogels (Fig. 5 B-b2). Due to the presence of fabric matrix, the hydrogel wound dressings avoided holistic breaking and falling off when overstretched. *In vivo* results demonstrated that the Fe_3O_4@C nanoparticles assembled hydrogel-functionalized textiles exhibited wound-healing effects and excellent antibacterial properties. Alternatively, antibiotics were applied for enhanced wound healing in combination with Ag NPs. For example, Ag NPs were synthesized using aqueous curcumin: hydroxypropyl-β-cyclodextrin complex and was loaded into bacterial cellulose hydrogel with moist wound-healing features, forming novel dressings with high cytocompatibility and antimicrobial activity against wound-infecting pathogenic microbes [170].

3.2.3. Photothermal induced wound healing

Considering potential advantage of PTT to induce minimal damage and high penetration of tissue triggered by NIR light, a large variety of photothermal nanoagents have been extensively exploited for wound healing application, while few studies focused on photothermal film (dry-type patch). Thus, in one design, plasmonic-induced photothermal cellulose-patch was fabricated as armored golden *E. coli* (AGE) microrods via fixing the hollow and spike-like gold nanostructures (Au NS) modified silica microrods on a unicellular organism [39]. Within this cellulose-patch, unicellular organism referred to as a framework, and silica microrods decorated with Au NS acted as plasmonic NPs, endowing it with excellent photothermal property with high photothermal conversion efficiency. Under NIR irradiation in a very short time, the surface temperature of such patch quickly increased to 264 °C, leading to superior desalination and sterilization, which showed the possible applicability for wound healing. As another typical plasmonic NPs, N,N-bis(acryloyl)-cystamine (BACA)-chelated Cu nanoparticles (Cu NPs) were applied to construct the composite hydrogel with

methacrylate-modified gelatin (Gel-MA) *via* radical polymerization with a photoinitiator [171]. Due to localized surface plasmon resonance (LSPR) effect of Cu NPs, such composite hydrogel patch was endowed with superior photothermal effect, resulting in predominant antibacterial efficacy against *S. aureus* and *E. coli* bacteria. Simultaneously, under NIR laser irradiation, heat produced from Cu NPs facilitated the rapid release of Cu^{2+}, triggering the fibroblast proliferation with no inflammatory responses. Such aforementioned synergistic effect providing the significantly accelerated would-healing with improved angiogenesis ability, prominent antibacterial effect, and decreased inflammatory response. Besides for plasmonic NPs as traditional photothermal nanoagents, other inorganic nanomaterials have also be considered as attractive photothermal dressings for enhancing antibacterial activities during infected wound healing. In a recent example of this, novel hydrogel scaffolds were fabricated to comprise of calcium silicate nanowires (CS), sodium alginate (SA), and oligomeric proanthocyanidins (OPC) enriched with flavonoids through a 3D printing method (Fig. 5C) [172]. Within such hydrogel scaffold, its superior and controlled photothermal effect were endowed by OPC due to grape-seed extracts, its rheological feature was varied with OPC amounts and irradiation time of NIR laser, as well as its compressive mechanical property could be regulated by different durations of NIR laser irradiation. Especially, under controlled NIR laser irradiation, OPC-containing hydrogel scaffolds could produce high heat and release metal ions like Si^{4+}, Ca^{2+}. Such synergic effect effectively induced the inhibition of melanoma-tumor growth and obviously improved the skin regeneration and angiogenesis of tumor-caused and chronic wounds, indicating this great potential of such NIR laser stimulative hydrogel scaffold in melanoma therapy and wound healing. Additionally, the combination of the PTT and antibiotic was also recently studied for promoted wound healing. For example, Guo et al. employed polydopamine-coated carbon nanotubes (CNT-PDA) to integrate with gelatin-grafted-dopamine (GT-DA) to fabricate GT-DA/chitosan/CNT composite hydrogels with conductive, antioxidant, adhesive and antibacterial properties via an oxidative coupling reaction of catechol groups based on a H_2O_2/HRP catalytic system [45]. For this design, the antibiotic doxycycline and CNT-PDA was respectively embedded into the hydrogels to endow them with antimicrobial activity and photothermal effect for effectively treating infected wound. *In vitro* data demonstrated such hydrogels were promising to be as multifunctional bioactive dressings for greatly healing wounds infected by bacteria.

3.2.4. Oxygen facilitated wound healing

To the best of our knowledge, oxygen played an important role in the process of wound healing through facilitating tissue remodeling and cell proliferation. Thus, to enhance the healing efficiency of wound, a wide diversity of oxygen carriers with good biocompatibility, flexibility and high oxygen-loading efficiency have been explored in the past few decades. Flexible polymeric matrixes, as common "drug" carriers, have been greatly studied to efficiently heal wound through directly inserting the deep parts of the skin in combination with integrating different NPs. Lately, separable responsive MNs integrated with black phosphorus quantum dots (BP QDs) and protein hemoglobin (Hb) was fabricated to carry oxygen and NIR-controlled oxygen delivery for wound healing, as shown in Fig. 5D [37]. In general, MNs were constructed of two parts: gelatin methacryloyl (GelMA) as the tip materials and polyvinyl acetate (PVA) as the backing layer, which were subsequently loaded with BP QDs and Hb. Based on fast dissolvability of PVA, the backing layers were soon disappeared and biocompatible tips were stayed inside the skin when applied to skin. Taking advantage of photothermal effect form BP QDs and the reversible oxygen-binding feature from Hb, the local temperature in skin could increase to induce the reduced binding capability between Hb and oxygen under the irradiation of NIR light, further gradually leading to responsively release oxygen, thus realizing the efficient wound healing. Of note, it is crucial to identify the highly efficient healing ability of BP QDs integrated MNs was demonstrated on

treating the cutaneous wounds of a type I diabetes on rat model. Such design indicated the potential value of such responsive NPs intercalated MNs in wound healing and other bioapplications.

3.3. Bone and cartilage regeneration

Except for the application in diabetic therapy and wound healing, flexible polymeric matrix hold the great potential for other diseases treatment including bone regeneration, cardiac constructs, hair growth, etc. owing to its good biocompatibility, relatively safe property and inherent minimal invasiveness. The incorporation of NPs into the polymeric matrix could lead to improve the mechanical and electrical features for obtaining satisfactory therapeutic efficacy. Thus, NPs intercalated flexible polymeric matrix has been broadly studied for improved therapy of treating these non-cancerous diseases.

Currently, bone tissue engineering has been mainly reported to explore novel active biomaterials that could induce the functional and structural interface with bone defect for remodeling the damaged tissues. Currently, a huge range of soft polymer materials have been widely applied for bone tissue engineering ascribed to biomineralization, biodegradability, biocompatibility, and osteogenic differentiation. The insertion of NPs simultaneously could endow polymeric matrix with comprehensive mechanical properties for improving bone and cartilage regeneration. To the best of our knowledge, polymeric hydrogels with self-healing properties have recently been received tremendous attention in tissue engineering applications because of the similar structure to the natural extracellular matrix.

Alternatively, it is widely acknowledged that the two-dimensional (2D) nanomaterial as a promising reinforcement material was commonly incorporated into polymeric matrix for next-generation bone tissue engineering application. As an example, Ding and his co-workers fabricated nanoengineered (NE) hydrogels with biomimetic extracellular matrices (ECM) microenvironments by incorporating ultrathin 2D black phosphorus (BP) nanosheets into the DN hydrogels with multiple

functions for tissue regeneration (Fig. 6A) [36]. Above all, this work firstly introduced poly(2-hydroxyethylacrylate) (PHEA), poly(N, N-dimethyl acrylamide) (PDMA), or polyacrylamide (PAM) as the first ductile network, and chitosan methacrylate (ChiMA), alginate methacrylate (AlgMA), or gelatin methacrylate (GelMA) as the second brittle network to form the combinatorial screening double network (DN) hydrogels with tunable strength through physically and chemically crosslinked networks *via* photopolymerization (Fig. 6A-a1). Notably, the as-chosen second brittle network was composed of methacrylate decorated natural-polymers originated from ECM molecules. Subsequently, synthetic exfoliated BP nanosheets were incorporated into various DN hydrogels with tunable toughness and high mechanical strength using a combinatorial screening strategy. It was noteworthy that the introduction of BP nanosheets facilitated the NE hydrogels for excellent bioactivity and exceptional mineralized matrix formation ability, which was beneficial for mediating cell fates and tissue regeneration of NE hydrogels. Beyond that, CaP nanocrystal in NE hydrogels were quickly generated under weak alkaline conditions with the assistance of BP nanosheets, thus which could mimic biological mineralization as the capability of CaP mineralization climbed in the NE hydrogels (Fig. 6A-a2). Collectively, the combination of bioactive components with excellent mechanical features improved the osteoblastic cell activity and bone regeneration in the NE hydrogels, exhibiting the great potential for regeneration of load-bearing tissues. Similarly, gelatin methacryloyl (GelMA) hydrogel matrix was applied to fabricate the physically and covalently conjugated nanocage-laden hydrogels through incorporating ferritin and equivalent apoferritin as nanocages [46]. Such hydrogels could release the loaded fluorescein isothiocyanate (FITC) by pH stimulus, showing the promising materials for bone repair engineering application. Lately, an acellular tissue patch (EHG) was explored using photo-induced imine crosslinking hydrogel glue with biocompatibility, superior operation ability and cartilage-integration as an exosome scaffold for cartilage regeneration [94]. Hereinto, such EHG was observed to exhibit the following features: the ability to positively
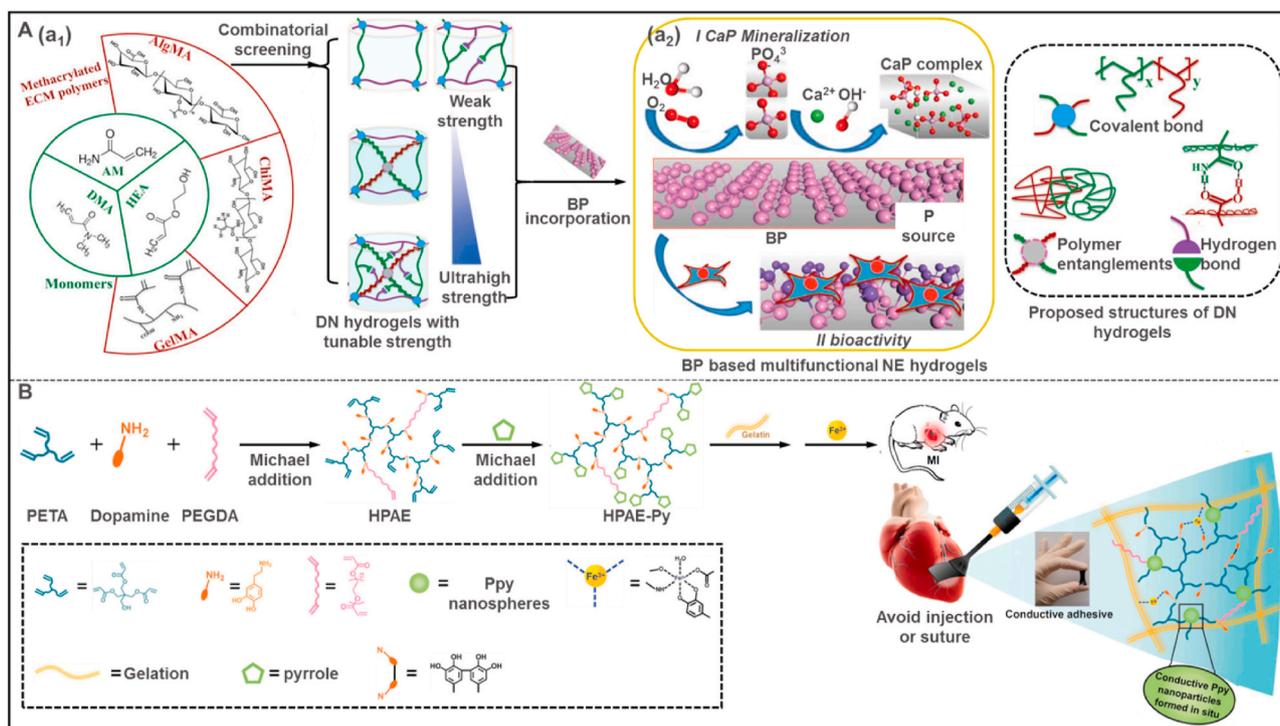

Fig. 6. A) Schematic illustration of BP NSs incorporated hydrogels for upregulated bone formation, **(a1)** illustrative preparation of double network (DN) hydrogels with different strength, **(a2)** bioactive nanoengineered (NE) hydrogels composition of black BP NSs and CaP matrix formation in DN hydrogels for bone regenerations. Reprinted with permission from Ref. [36]. Copyright 2019, Wiley. **B)** Scheme for preparing a conductive and adhesive hydrogel for painting directly on the surface of MI heart in SD rats. Reprinted with permission from Ref. [64]. Copyright 2018, Wiley.

adjust chondrocytes and hBMSCs in vitro with reserving SC-Exos; improving the capability of cell deposition at cartilage defect sites through integrating with native cartilage matrix which thus facilitating the enhancement of cartilage defect repair. This result indicating the potential of EHG tissue patch as cell-free scaffold material for future wound repair. Also, KGN-loaded PLGA NPs was developed to integrate with m-HA hydrogel for facilitating hyaline cartilage and subchondral bone tissue repair [173].

Except for polymeric hydrogel patches, other structured polymeric patches have also emerged as a feasible non-invasive matrix for bone and cartilage regeneration. In a recent example of this, PCL/zein/MoS₂ (PZM) composite nanofibrous scaffolds were developed through embedding 2D MoS_2 nanosheets into polycaprolactone (PCL)/zein (PZ) composite polymeric network based on an electrospinning method [38]. This scaffolds possessed superior biocompatibility, excellent cell attachment, proliferation and differentiation behavior, proving their potential to apply in bone tissue engineering. It has been reported that cartilage regeneration scarcely exhibited innate self-healing ability, which is still currently a great challenge in clinic. Stem cell-derived exosomes (SC-Exos) has emerged as an emerging extracellular nano-vesicle for cartilage regeneration to replace stem cell-based treatment. Beyond that, polypyrrole nanoparticles (Ppy-NPs) were applied to incorporate into PCL polymeric matrix for building nanofibrous scaffolds *via* a low-cost facile strategy [124]. Such PCL/PPy conductive scaffolds could improve the behavior of biocompatibility, bioactivity, and osteogenic differentiation through stimulating by electric, indicating the potential for bone tissue engineering application. Besides, in a more effective paradigm, a series of mechanically activated microcapsules (MAMCs) were designed as a stimuli-triggered delivery system for tissue engineering application [174]. Specially, such mechanical regulation of microcapsules was designed to be as a technique for eliciting tissue repair and regeneration. Thus, inspired by self-healing polymer systems, microcapsules intercalated in a polymer matrix could be disrupted to release the loaded drug upon physical damage. More important, the feasibility of encapsulating transforming growth factor-*β3* (TGF-*β3*) within biocompatible and biodegradable MAMCs was realized for promoting tissue formation through microenvironment modulated mechano-activation. Such design demonstrated a novel strategy for regenerating injured musculoskeletal tissues in mechanical loading environment.

3.4. Cardiac constructs and repairs

Myocardial infarction (MI) is well-known one of the most common causes of disability and death in the world. To days, with the development of nanotechnology in medicine, many different sorts of strategies has widely explored for the treatment of MI, such as cardiac patches and injectable biomaterials. The therapeutic efficacy of most approaches is limited by a single method. To improve the efficacy of MI treatment, synergistic therapy strategy was increasingly designed in the recent years. For example, an injectable hydrogel and conductive hydrogel patch was proposed as a combined therapy method for co-administration into the infarcted myocardium [97]. In this system, such conductive patch composed of Fe^{3+}-induced ionic coordination between dopamine-functionalized polypyrrole (DA-PPy) and dopamine-gelatin (GelDA) conjugates was painted on the heart surface, and subsequently cleavable hydrogel in situ formed based on a Schiff base reaction between hydrazided hyaluronic acid (HHA) and oxidized sodium hyaluronic acid (HA-CHO) was intramyocardially injected. Such combined protocol induced a great enhancement of the cardiac function through histological, echocardiographical, and angiogenic outcomes in comparison with a single-mode system. A similar exemplary study in this regard was designed by Liu and his colleagues. A biocompatible paintable conductive hydrogel was designed as cardiac patches for the treatment of MI through Fe^{3+}-triggered simultaneous in situ polymerization of Ppy and dopamine (Fig. 6B) [64]. The Ppy as a unique crosslinker was chemically linked to hyperbranch polymer chains to stabilize the network and endow the gels formed with conductivity. Such resultant conductive and adhesive hydrogel had the capability of conveniently painting as a patch and rapidly bonding onto the beating heart surface owing to dopamine-Fe^{3+} coordination with no adverse liquid leakage. Such functional patch with similar conductivity to normal myocardium showed the strong bonding to heart for around one month, thus efficiently and increasing the conduction of electrophysiological signals. Besides this, revascularization of MI and the reconstruction of cardiac function exhibited the remarkable improvement. All in all, the translatable suture-free cardiac patch designed in this work has the potential for clinical challenges in cardiac tissue engineering.

As is previous demonstrated, it is most important for biomimetic scaffolds for engineered cardiac constructs to improve function of the cardiomyocytes (CMs), such as conductivity, mechanics, and sub-micrometer structure of the matrix. Thus, lately, carbon nanotubes (CNTs) were chosen to combine with hydrogel for improving cardiac construct. In a simple paradigm, type I collagen hydrogels was integrated with CNTs to form hybrid hydrogel matrix with potentially improved hydrogel strength and conductivity [175]. In comparison with those within pure collagen hydrogels, the result of cardiomyocytes (CMs) treated by the CNT-collagen hybrid hydrogels revealed the enhancement of cardiac cell functions, indicating the great potential of such hybrid hydrogel as biomimetic scaffold for engineered cardiac construct. In another similar example, Khademhossein et al. integrated CNTs with photo-cross-linkable gelatin methacrylate (GelMA) hydrogels to form functional cardiac patches with superior mechanical integrity and enhanced electrophysiological functions through seeding neonatal rat cardiomyocytes [48]. Compared with pristine GelMA hydrogels, CNT-GelMA treated myocardial tissues not only have 85% lower excitation thresholds, but also showed 3 times higher spontaneous synchronous beating rates. The incorporation of CNT within a porous gelatin framework caused the electrically conductive and nanofibrous networks, resulting in optimized cardiac cell adhesion, organization, and cell-cell coupling. The formation of 3D biohybrid actuators released from patches exhibited the controllable linear cyclic contraction/extension, pumping, and swimming actuations. CNT-GelMA cultured cardiac tissues circumvented damage from a cytotoxic compound and a model cardiac inhibitor. Consequently, combination of CNTs into gelatin is promising for neuron and other muscle cells to design multifunctional cardiac constructs with optimized electro-activity, organization, and mechanical integrity.

It is well-known that the deprivation of oxygen could cause ischemic heart disease, further inducing the progressive loss and apoptosis of cardiac cells. Thus, oxygen is prerequisite for tissue function and cell survival. Taking advantages of MI, as-generated ischemia leads to tissue necrosis and cell death. Many approaches to regenerate myocardial tissue could intensify the hypoxic stress accompanying with the increased metabolic burden. Therefore, implanted cardiac tissues generally produced hypoxia-induced cell death. Currently, oxygen-self-supplying hydrogels was designed through loading calcium peroxide (CPO) into gelatin methacryloyl (GelMA) [47]. Under hypoxic conditions (1% O_2), such hydrogels was observed to gradually release amount of oxygen in 5 days, which is enough to alleviate the metabolic stress from cardiac cells. Particularly, incorporation of CPO in GelMA hydrogels greatly improved cell viability, which is due to that oxygen generation from CPO could reduce cell apoptosis that limited by hypoxia-induced necrosis. Good result was obtained when used such hydrogel to cardiac cells under ischemic conditions. In consequence, this CPO-GelMA can provide an alternative way to improve the regeneration or treatment of infarcted myocardial tissue.

3.5. Dermatological disease therapy

With the development of nanomedicine, dermatological disease has attracted tremendous attention owing to their advantages of high

prevalence and visible symptoms [176,177]. Currently, flexible polymeric patch has also been extensively applied for diverse skin diseases treatment including actinic keratosis, scars, and acne, etc. [178] For instance, Lotti et al. utilized polymeric MN patches to effectively suppress atrophic acne scar without any severe complication and post-inflammatory hyperpigmentation through enhancing skin roughness and pigmentation spots in patients. Xu's group fabricated a self-administered and drug-free MN patch for effectively inhibiting the abnormal scars post-injury [179]. Currently, by integrating nanomaterials, the polymeric patches could effectively enhance the therapy efficacy of dermatological disease. Retinoids are known to reduce signs of skin aging and improve smooth atrophic acne scars. Frequently, Retinoids were typically applied for improving several skin conditions. As a natural precursor of retinoic acid, retinal could exert the biological activities of retinoids and is beneficial for the treatment of photoaging [180] and acne scarring. Like Patzelt's report, proretinal nanoparticles (PRN) were combined to efficiently deliver retinal for realizing direct dermis targeting [181]. When applied MNs patches, PRN could be loaded and accumulated in the microchannels of skin, as well as recovered retinal concentration in the dermis was obviously higher in comparison with conventional retinal and PRN solution.

Hypertrophic scar (HS) is acknowledged to be an abnormal tissue condition caused by burns, injuries, and surgical wounds, which was embodied by a raised, inflamed, and red surface. Usually, HS could produce pruritus, pain, and skin tightening, accompanying by a series of psychological, physical, and cosmetic problems. As one of the most common therapeutics of HS, polymeric patches based drug delivery could enable self-administration, painlessness, good bioavailability, and the fast onset of action. As an attractive paradigm, dissolving MNs were fabricated by hyaluronic acid (HA) to load bleomycin for improved efficient suppression of hypertrophic scars [182]. Such system possessed some superior features of the rapid dissolution of MN to release bleomycin in short time, the recovery of MN treated skin to its sufficient mechanical strength, original status to pierce porcine skin *ex vivo*, and the protection of stability and activity of bleomycin from HA matrix, leading to its promising feasibility for treating HS. Through in vitro experiment, this method could efficiently prevent the proliferation of human hypertrophic scar fibroblasts (hHSFs) and the secretion of transforming growth factor-*b* (TGF-*b1*), showing the potential of this stratagem for HS therapy in an efficient, convenient, and minimally invasive manner. In another similar example, hydroxypropyl-β-cyclodextrin (HP-β-CD) and sodium hyaluronic acid (HA) were applied to build a dissolving MN with improved loading triamcinolone acetonide (TA) for treating HS [183]. Specially, through delivering TA to HS site by MN, mRNA expressions of Collagen I and transforming growth factor-$\beta1$ (TGF-$\beta1$) were down-regulated to normal, indicating the potential of such system as a convenient and low-pain therapeutic strategy for treating HS. Alternatively, except for drug, some nucleic acids like small interfering RNA (siRNA) also could be loaded and delivered by MNs into skin tissue. Due to some challenges during the delivered siRNAs process including the enzymatic degradation, the difficulty to enter target cells, and the easy leakage from the endosome-lysosome degradation, Xu's group used dissolvable HA as the polymeric matrix and mesoporous silica-coated upconversion nanoparticles (UCNPs@mSiO$_2$) as the siRNA depot to design a nanoparticle-embedding MN system [184]. Under the help of upconversion luminescence imaging or optical coherence tomography (OCT) imaging of UCNPs, the process of MN skin penetration and NP diffusion could be tracked and clearly observed. Through protecting and loading molecular beacons (MBs) and siRNA of SiO$_2$, the targeting transforming growth factor-beta type I receptor (TGF-βRI) could be decreased, implying the potential of this system for abnormal scar treatment.

Acne vulgaris is one of the most common chronic inflammatory skin disorders. It is associated with a colonization of bacterium propionibacterium acnes (*P. acnes*), whose rapid growth could cause metabolic byproducts, cellular damage and bacterial debris to exacerbate the inflammation reaction, thus leading to the psychological and physiological impact to the patients. Despite the strategy using antibiotic cream was developed for acne treatment, low delivery efficiency of drug to bacterium pilosebaceous infected lesions caused poor therapy efficiency. Lately, Gu et al. explored a ROS-responsive MN patch for efficiently treating acne vulgaris through improving the interaction of antibiotics with bacterial (Fig. 7A) [185]. Concretely, during preparing MNs patch process, a methacrylated hyaluronic acid (m-HA)/diatomaceous earth (DE) was integrated as the supporting substrate for promoted healing, and drug-loaded ROS-responsive poly(vinyl alcohol) (RR-PVA) was utilized as the matrix to catch clindamycin (CDM) to form RR-PVA/CDM gel for *P. acnes* elimination. Under the trigger of ROS (high concentration of H$_2$O$_2$), RR-PVA gel was quickly degraded to release CDM within the P. acnes-infected lesions in controlled and sustained drug release manner after penetrating through epidermis, leading to the effective inhibition of bacteria proliferation with reduced the side effects. Due to the high physical adsorption capability of HA and DE, this patch enabled to accelerate healing of skin through absorbing pus and dead cell debris. Additionally, in vivo experiment realized such bioresponsive patch had the ability to efficiently decrease the skin swelling and ablate bacterial, indicating its promising to treat various other skin diseases.

3.6. Hair loss therapy

Hair loss is known as a common disorder in humans from diseases, aging, and medications. On account of the social and psychological impacts, increasing population suffered from hair loss. Currently, hair follicle transplantation was main strategy for clinical treatment of hair loss, for example, valproic acid (VPA), a food and Drug Administration (FDA)-approved anticonvulsant drug, was encapsulated into dissolving MN patch to effectively stimulate hair follicle (HF) regrowth by up-regulating Wnt/b-catenin for hair loss therapy [187]. However, this application was limited because of donors' shortage as well as costly and invasive surgery. Additionally, it is promising for hair loss therapy to promote hair follicle regrowth through activating hair follicle stem cells (HFSCs), while some challenges still existed. To enhance the delivery efficiency of hair loss drugs, enable the easy administration and extend the retention of exosomes for hair regrowth, Gu's group fabricated a detachable MN patch based drug delivery system for sustained delivery of HFSC activators to heal hair loss (Fig. 7B) [77]. Herein, such MN patch based system included three parts: hair-derived keratin based hydrogel covered by an HA-based patch, mesenchymal stem cell (MSC)-derived exosomes and UK5099 as the HF stem cells (HFSC) activator loaded into PLGA NPs. Upon administration in hair loss C57BL/6J mouse models, this MN patch based drug delivery system exhibited the improved hair regrowth and pigmentation within 6 days with enhanced curative effect even at a reduced dosage. In short, this polymeric patch had the great potential for hair loss therapy in comparison with subcutaneously injecting exosomes and administrating UK5099.

3.7. Obesity therapy

Obesity is one of the most serious public health issues, which could induce various serious associated disorders, including cancer, cardiovascular diseases, and type-2 diabetes. Currently, all sorts of therapy approaches towards obesity, such as diet, pharmacological therapy, physical exercise, and surgeries were limited by undesired side effects or low effectiveness. Currently, the most common approach to treat obesity is oral medications, which could be capable to inhibit fat absorption and suppress appetite through acting on the gastrointestinal tract and central nervous system. However, such traditional strategy could possibly lead to high side effects and poor effectiveness. Thus, to improve the therapeutics efficiency of obesity with reduced side effects, nanomaterials encapsulating anti-obesity drugs integrated with polymeric patches
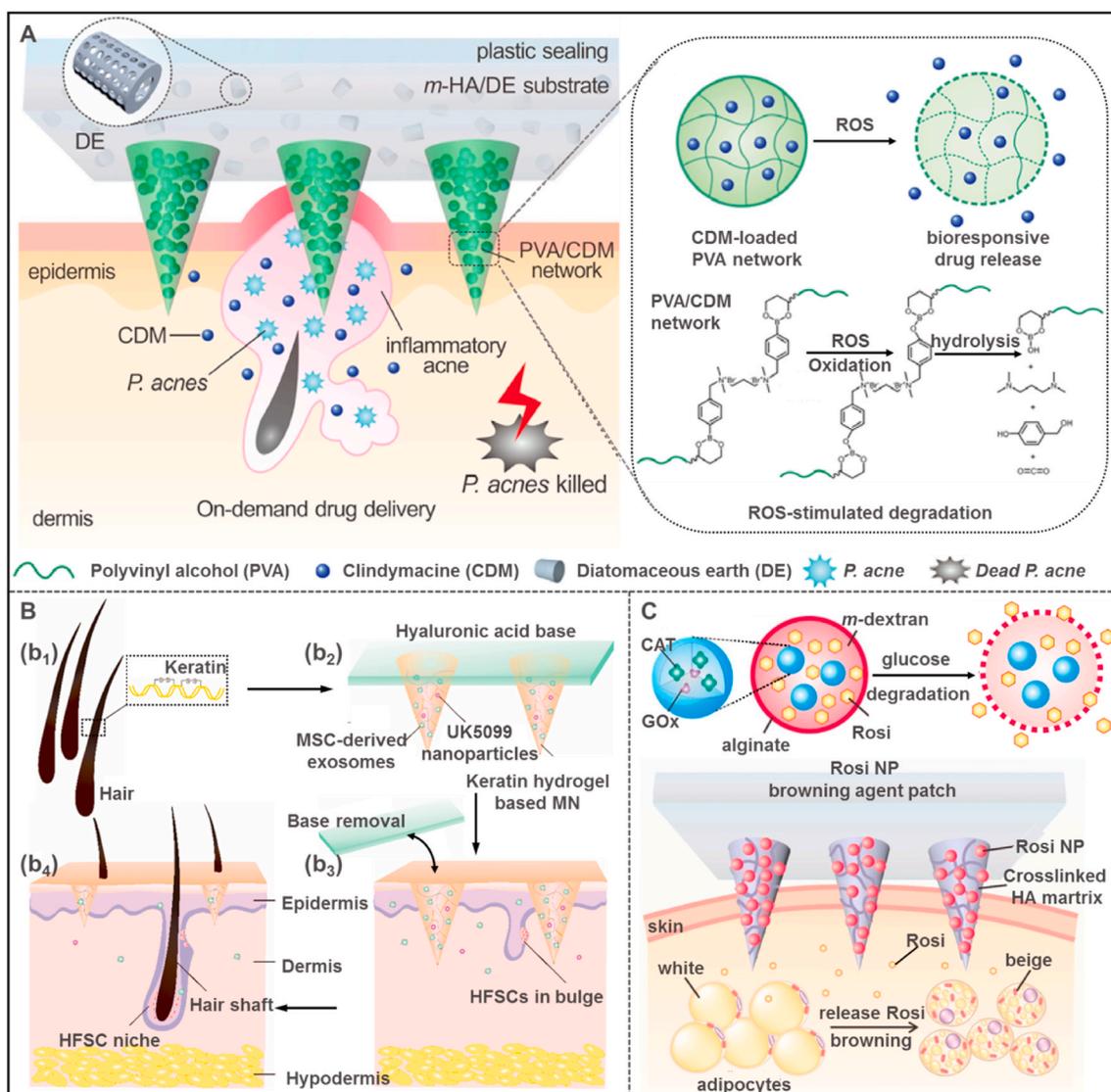
Fig. 7. A) Illustrative fabrication and mechanism of a ROS-responsive microneedle patch for acne vulgaris treatment. Reprinted with permission from Ref. [185]. Copyright 2018, Wiley. **B)** Schematic of a detachable microneedle patch for hair loss therapy, **(b1)** illustrative depiction of Keratin that used to form the polymeric matrix of MNs, **(b2)** schematics of keratin hydrogel-based MNs encapsulated with MSC-derived exosomes and UK5099-loaded PLGA NPs, **(b3)** illustrative process of MNs applying to the skin for sustained release of therapeutics, **(b4)** schematic description of transdermal delivery of HFSC for accelerating a new hair cycle transition and hair regrowth. Reprinted with permission from Ref. [77]. Copyright 2019, American Chemical Society. **C)** Schematic illustration of transcutaneous MN patch loaded with NPs comprised of Rosi, GOx, CAT and pH-sensitive acetal-modified dextran for the brown remodeling of the white fat. Reprinted with permission from Ref. [186]. Copyright 2017, American Chemical Society.

have been widely developed for obesity therapy. As an exemplary work, a NPs integrated MN patch was fabricated to locally brown the white adipose tissue (WAT) for obesity therapy, as depicted in Fig. 7C [186]. In such system, NPs were formed through encapsulating GOx, CAT, rosiglitazone (Rosi) as an agonist of peroxisome proliferator-activated receptor gamma (PPARγ) and pH-sensitive acetal-modified dextran under alginate coating. Subsequently, NPs were further integrated with MN patches consisted of HA matrix for the brown remodeling of the white fat. In brief, with the help of the physiological glucose concentration, GOx could produce gluconic acid to decrease the local pH and CAT consumed H_2O_2 from the GOx-medicated enzymatic reaction, leading to degrade NPs to release Rosi for WAT browning. *In vivo* experiments in a diet-induced obesity mouse model demonstrated to increase the energy expenditure and fatty acid oxidation, effectively control body weight through reducing treated fat pad size, showing polymeric patches were promising for clinical treatment of obesity. Besides for this, stimuli-hydrogels are also recently explored for highly effectively

treating obesity combined with nanomaterials. Recently, Chen's group incorporated copper sulfide nanodots (CuS-ND) into injectable thermo-responsive hydrogel to induce the ameliorating remodeling based on directly acting on the root of evil according to transdermal mild photothermal therapy [188]. Simultaneously, mirabegron was further co-delivered with such hydrogels, inducing a strong therapeutic synergy. Therefore, this synergistic therapy system realized both high effectiveness and low side effect by virtue of targeted and localized application. In particular, in vivo CuS-ND embedded hydrogel treated high-fat-diet fed mice was found to show the reduced serum levels of triglyceride/insulin/cholestero/glucose, decreased masses and improved insulin sensitivity, proving the high insights to explore effective approaches to inhibit obesity and the associated metabolic disorders.

3.8. Immune disease therapy

An autoimmune disease is the result of the immune system accidently attacking your body instead of protecting it. It's still unclear why the immune system does this. With the development of socioeconomics, a rising number of immune diseases including rheumatoid arthritis, hashimoto's autoimmune thyroiditis, graves' disease, celiac disease, rheumatic fever, vitiligo, etc. came out to bring a threat to human health. Up to now, various strategies have been studied for improving antigen immunogenicity. Particularly, a plenty of nanomaterials was introduced to load antigen [189], vaccines [190] and DNA [67,191, 192], and then inserted in polymeric patches for vaccination. Giving an example, Duong et al. fabricated a nanopolyplex using cationic amphiphilic conjugates with ovalbumin-expressing plasmid OVA (pOVA) and immunostimulant-polyinosinic:polycytidylic acid (poly(I:C)) to mix with bioresorbable polypeptide matrix to form dissolving MN cocktails [193]. Compared with MN-free nanopolyplex and traditional vaccination, such MN cocktails induced a stronger antigen-specific antibody response and increased the antibody recall memory after challenge.

Various DNA vaccines that were loaded into nanomaterials and intradermally delivered by polymeric patches have also been investigated. polylactic-co-glycolic acid-poly-l-lysine/poly-γ-glutamic acid (PLGA-PLL/γPGA) nanoparticles were applied to load a DNA vaccine and integrate with MN patch for Ebola vaccination [67]. In such system, MN patch made vaccine administration minimize trained personnel, while nanoparticles kept vaccine stability even no refrigeration. This study showed a potential strategy for Ebola vaccination for some developing countries where Ebola is most prevalent. In another example, Liao and coworkers designed DNA polyplex vaccine and combined it with MN patches to cause the high immunogenicity via intradermal vaccination and the enhanced vaccine stability during storage outside the cold chain [191]. This system induced stronger immune response, and provided superior vaccine stability at high temperature, indicating its significance to public health and effective vaccination in developing countries. Similarly, DNA was condensed to form cationic nanoparticles by a peptide RALA, which was further integrated with MN patches to build a 'smart system' platform for DNA vaccination against cervical cancer [192].

Presently, COVID-19, as a new immune disease, has been prevalent in the world and produced tremendous influence on human life. Although different vaccines toward COVID-19 are always in studying, more approaches were urgent to be developed for effective vaccination. For example, a fingertip-sized patch of needles was being studied to deliver a recombinant protein as the antigen into the skin. Within this context, the nanomaterials integrated polymeric patches showed the probability to be applied in this vaccine against COVID-19.

4. Conclusion and perspectives

In conclusion, polymeric patches with special flexibility, especially MNs and hydrogel, have attracted great research interests as an attractive therapeutic system against non-cancerous disease with inherent minimal invasive and relatively safe features because of good biocompatibility, superior biodegradation, and high loading capability. Except this, flexible polymeric matrixes embodied more advantages just like the optimized patient compliance, controllable drug release, and improved loading efficiency and permeability of drug, facilitating their extensive application in biomedicine. Though integrating the nanomaterials and flexible polymeric patches, these flexible polymeric systems against noncancer treatment were rendered to endow with these synergistic merits of lowered systemic side effects and enhanced therapeutic efficacy. Therefore, we herein systematically summarized that various nanomaterials incorporated polymeric patches were explored as a safe and effective therapeutic vehicle for treating non-cancerous diseases, such as diabetes therapy, wound healing, dermatological disease therapy, bone regeneration, cardiac repair, hair repair and obesity therapy.

However, in spite of the latest exciting outcomes from nanomaterial integrated polymeric patches for non-cancerous diseases therapy, several challenges and limitation still remained that need to be developed before further clinical translations: (I) the insertion of nanomaterials renders the impact on the mechanical strength of polymeric matrixes; (II) the reliable and principled strategy is limited to accurately reduce the bioavailability of this polymeric system, thus lowering the future clinical translation; (III) the incorporated nanomaterials facilitates the complexity of polymeric patches synthesis; (IV) the characterized methods regarding biosafety of nanomaterials and polymeric matrixes should be performed; (V) most incorporated nanomaterials still exist the long-term biodegradability and clearance of from the body.

To raise the solution to these issues, novel nanomaterials incorporated polymer patches with improved chemical, physical and optoelectronic performances regarding therapy as well as superior biocompatibility should be fabricated to meet the specific demands of therapeutics against non-cancerous deceases. Therein, some polymeric matrixes with excellent biodegradability or dissolvability, high biocompatibility, and high drug-loading capability should be designed and developed into flexible patches to encapsulate or modify nanomaterials with amplified therapy efficiency. Additionally, some tailored nanomaterials with special features including ultrasonic, magnetothermal, photoacoustic, chemodynamic, photothermal, and photodynamic effect should be widely explored to realize multi-modal therapeutics against non-cancerous diseases. Anything but this, to retain the inherent properties of the inserted nanomaterials and prevent the interplay between nanomaterials and polymeric matrixes, appropriate nanomaterials as active therapeutic components and soft matrix materials as polymeric templates should be designed to be tailored and coordinated. Particularly, to facilitate the development of treating human diseases like cancer, diabetes, abnormal scars and obesity, an increasing exploration should be given on microscale synthesis of nanomaterials integrated polymeric patch in association with delivery systems. Last but not least, it should pay more attention for the biosafety and bioavailability of both polymeric matrixes and nanomaterials to reduce systemic toxicity.

In a word, despite the nanomaterials combined polymeric patch systems have proven to be promising for understanding fundamental therapeutics with enhanced curative treatment, next generation's polymeric patches incorporated by a diversity of novel nanomaterials with multi-functionality are till necessary to explore more application in biomedicine. Furthermore, further clinical translation of nanomaterials based polymeric patches with minimal invasion and cost-effect would be urgently explored for bringing more convenience to patient's life.

CRediT authorship contribution statement

Houjuan Zhu: Writing – original draft, preparation. **Justin Mah Jian Qiang:** Writing – original draft, co-writing the original draft. **Chen Gang Wang:** Writing – original draft, co-writing the original draft. **Chui Yu Chan:** Writing – original draft, co-writing the original draft. **Qiang Zhu:** Writing – original draft, co-writing the original draft. **Enyi Ye:** Writing – review & editing, Writing – review & editing. **Zibiao Li:** Writing – review & editing, Writing – review & editing. **Xian Jun Loh:** Conceptualization, Writing – review & editing.

Declaration of competing interest

The authors declare no conflict of interest, financial or otherwise.

Acknowledgment

References

[1] S. Henry, D.V. McAllister, M.G. Allen, M.R. Prausnitz, Microfabricated microneedles: a novel approach to transdermal drug delivery, J. Pharmacol. Sci. 88 (9) (1999) 948.

[2] T.M. Tuan-Mahmood, M.T. McCrudden, B.M. Torrisi, E. McAlister, M.J. Garland, T.R. Singh, R.F. Donnelly, Microneedles for intradermal and transdermal drug delivery, Eur. J. Pharmaceut. Sci. 50 (5) (2013) 623–637.

[3] K. Sigfridsson, A.J. Lundqvist, M. Strimfors, Particle size reduction for improvement of oral absorption of the poorly soluble drug UG558 in rats during early development, Drug Dev. Ind. Pharm. 35 (12) (2009) 1479–1486.

[4] A. Shahiwala, Formulation approaches in enhancement of patient compliance to oral drug therapy, Expet Opin. Drug Deliv. 8 (11) (2011) 1521–1529.

[5] H. Zhu, N. Ni, S. Govindarajan, X. Ding, D.T. Leong, Phototherapy with layered materials derived quantum dots, Nanoscale 12 (1) (2020) 43–57.

[6] P.H. Cheng, P. Chen, K. Pu, Recent progress in the development of near-infrared organic photothermal and photodynamic nanotherapeutics, Biomater. Sci. 6 (4) (2018) 746–765.

[7] X. Lan, J. She, D.A. Lin, Y. Xu, X. Li, W.F. Yang, V.W.Y. Lui, L. Jin, X. Xie, Y.X. Su, Microneedle-mediated delivery of lipid-coated cisplatin nanoparticles for efficient and safe cancer therapy, ACS Appl. Mater. Interfaces 10 (39) (2018) 33060–33069.

[8] Z. Zhang, J. Wang, C. Chen, Near-infrared light-mediated nanoplatforms for cancer thermo-chemotherapy and optical imaging, Adv. Mater. 25 (28) (2013) 3869–3880.

[9] H. Zhu, Z. Lai, Y. Fang, X. Zhen, C. Tan, X. Qi, D. Ding, P. Chen, H. Zhang, K. Pu, Ternary chalcogenide nanosheets with ultrahigh photothermal conversion efficiency for photoacoustic theranostics, Small 13 (16) (2017).

[10] C. Wang, X. Wang, K. Dong, J. Luo, Q. Zhang, Y. Cheng, Injectable and responsively degradable hydrogel for personalized photothermal therapy, Biomaterials 104 (2016) 129–137.

[11] J. Shao, H. Xie, H. Huang, Z. Li, Z. Sun, Y. Xu, Q. Xiao, X.F. Yu, Y. Zhao, H. Zhang, H. Wang, P.K. Chu, Biodegradable black phosphorus-based nanospheres for in vivo photothermal cancer therapy, Nat. Commun. 7 (2016) 12967.

[12] H. Zhu, Z. Li, E. Ye, D.T. Leong, Oxygenic enrichment in hybrid ruthenium sulfide nanoclusters for an optimized photothermal effect, ACS Appl. Mater. Interfaces 13 (50) (2021) 60351–60361.

[13] H. Zhu, Y. Fang, Q. Miao, X. Qi, D. Ding, P. Chen, K. Pu, Regulating near-infrared photodynamic properties of semiconducting polymer nanotheranostics for optimized cancer therapy, ACS Nano 11 (9) (2017) 8998–9009.

[14] J. Ge, M. Lan, B. Zhou, W. Liu, L. Guo, H. Wang, Q. Jia, G. Niu, X. Huang, H. Zhou, X. Meng, P. Wang, C.S. Lee, W. Zhang, X. Han, A graphene quantum dot photodynamic therapy agent with high singlet oxygen generation, Nat. Commun. 5 (2014) 4596.

[15] X. Ding, F. Peng, J. Zhou, W. Gong, G. Slaven, K.P. Loh, C.T. Lim, D.T. Leong, Defect engineered bioactive transition metals dichalcogenides quantum dots, Nat. Commun. 10 (1) (2019) 41.

[16] F. Zhang, F. Li, G.H. Lu, W. Nie, L. Zhang, Y. Lv, W. Bao, X. Gao, W. Wei, K. Pu, H. Y. Xie, Engineering magnetosomes for ferroptosis/immunomodulation synergism in cancer, ACS Nano 13 (5) (2019) 5662–5673.

[17] S. He, Y. Jiang, J. Li, K. Pu, Semiconducting polycomplex nanoparticles for photothermal ferrotherapy of cancer, Angew Chem. Int. Ed. Engl. 59 (26) (2020) 10633–10638.

[18] L.H. Fu, Y.R. Hu, C. Qi, T. He, S. Jiang, C. Jiang, J. He, J. Qu, J. Lin, P. Huang, Biodegradable manganese-doped calcium phosphate nanotheranostics for traceable cascade reaction-enhanced anti-tumor therapy, ACS Nano 13 (12) (2019) 13985–13994.

[19] K. Hu, J. Sun, Z. Guo, P. Wang, Q. Chen, M. Ma, N. Gu, A novel magnetic hydrogel with aligned magnetic colloidal assemblies showing controllable enhancement of magnetothermal effect in the presence of alternating magnetic field, Adv. Mater. 27 (15) (2015) 2507–2514.

[20] C.Y. Wang, N.Y. Zhao, Y.X. Huang, R. He, S.C. Xu, W.Z. Yuan, Coordination of injectable self-healing hydrogel with Mn-Zn ferrite@ mesoporous silica nanospheres for tumor MR imaging and efficient synergistic magnetothermal-chemo-chemodynamic therapy, Chem. Eng. J. 401 (2020) 126100.

[21] Q. Chen, C. Wang, X. Zhang, Q. Hu, H. Li, J. Wang, D. Wen, Y. Zhang, Y. Lu, G. Yang, C. Jiang, G. Dotti, Z. Gu, In situ sprayed bioresponsive immunotherapeutic gel for post-surgical cancer treatment, Nat. Nanotechnol. 14 (1) (2019) 89–97.

[22] C. Wang, Y. Ye, G.M. Hochu, H. Sadeghifar, Z. Gu, Enhanced cancer immunotherapy by microneedle patch-assisted delivery of anti-PD1 antibody, Nano Lett. 16 (4) (2016) 2334–2340.

[23] M.A. Lopez-Ramirez, F. Soto, C. Wang, R. Rueda, S. Shukla, C. Silva-Lopez, D. Kupor, D.A. McBride, J.K. Pokorski, A. Nourhani, N.F. Steinmetz, N.J. Shah, J. Wang, Built-in active microneedle patch with enhanced autonomous drug delivery, Adv. Mater. 32 (1) (2020), e1905740.

[24] G. Song, L. Cheng, Y. Chao, K. Yang, Z. Liu, Emerging nanotechnology and advanced materials for cancer radiation therapy, Adv. Mater. 29 (32) (2017) 1700996.

[25] M.R. Gill, K.A. Vallis, Transition metal compounds as cancer radiosensitizers, Chem. Soc. Rev. 48 (2) (2019) 540–557.

[26] P. Majumder, U. Baxa, S.T.R. Walsh, J.P. Schneider, Design of a multicompartment hydrogel that facilitates time-resolved delivery of combination therapy and synergized killing of glioblastoma, Angew Chem. Int. Ed. Engl. 57 (46) (2018) 15040–15044.

[27] J. Conde, N. Oliva, Y. Zhang, N. Artzi, Local triple-combination therapy results in tumour regression and prevents recurrence in a colon cancer model, Nat. Mater. 15 (10) (2016) 1128–1138.

[28] L. Zhou, J. Zhao, Y. Chen, Y. Zheng, J. Li, J. Zhang, Y. Liu, X. Liu, S. Wang, MoS2-ALG-Fe/GOx hydrogel with Fenton catalytic activity for combined cancer photothermal, starvation, and chemodynamic therapy, Colloids Surf. B Biointerfaces 195 (2020) 111243.

[29] J. Wang, F. Tang, Y. Wang, Q. Lu, S. Liu, L. Li, Self-healing and highly stretchable gelatin hydrogel for self-powered strain sensor, ACS Appl. Mater. Interfaces 12 (1) (2020) 1558–1566.

[30] R. Xing, K. Liu, T. Jiao, N. Zhang, K. Ma, R. Zhang, Q. Zou, G. Ma, X. Yan, An injectable self-assembling collagen-gold hybrid hydrogel for combinatorial antitumor photothermal/photodynamic therapy, Adv. Mater. 28 (19) (2016) 3669–3676.

[31] W. Xie, Q. Gao, Z. Guo, D. Wang, F. Gao, X. Wang, Y. Wei, L. Zhao, Injectable and self-healing thermosensitive magnetic hydrogel for asynchronous control release of doxorubicin and docetaxel to treat triple-negative breast cancer, ACS Appl. Mater. Interfaces 9 (39) (2017) 33660–33673.

[32] E.J. Cho, B. Sun, K.O. Doh, E.M. Wilson, S. Torregrosa-Allen, B.D. Elzey, Y. Yeo, Intraperitoneal delivery of platinum with in-situ crosslinkable hyaluronic acid gel for local therapy of ovarian cancer, Biomaterials 37 (2015) 312–319.

[33] M.C. Chen, M.H. Ling, K.W. Wang, Z.W. Lin, B.H. Lai, D.H. Chen, Near-infrared light-responsive composite microneedles for on-demand transdermal drug delivery, Biomacromolecules 16 (5) (2015) 1598–1607.

[34] Y. Ye, J. Wang, Q. Hu, G.M. Hochu, H. Xin, C. Wang, Z. Gu, Synergistic transcutaneous immunotherapy enhances antitumor immune responses through delivery of checkpoint inhibitors, ACS Nano 10 (9) (2016) 8956–8963.

[35] C.H. Park, T. Kim, G.H. Lee, K.H. Ku, S.H. Kim, B.J. Kim, Fluorescent polymer-MoS2-embedded microgels for photothermal heating and colorimetric monitoring, ACS Appl. Mater. Interfaces 12 (31) (2020) 35415–35423.

[36] Z. Wang, J. Zhao, W. Tang, L. Hu, X. Chen, Y. Su, C. Zou, J. Wang, W.W. Lu, W. Zhen, R. Zhang, D. Yang, S. Peng, Multifunctional nanoengineered hydrogels consisting of black phosphorus nanosheets upregulate bone formation, Small 15 (41) (2019), e1901560.

[37] X. Zhang, G. Chen, Y. Liu, L. Sun, Y. Zhao, Black phosphorus-loaded separable microneedles as responsive oxygen delivery carriers for wound healing, ACS Nano 14 (5) (2020) 5901–5908.

[38] G.P. Awasthi, V.K. Kaliannagounder, B. Maharjan, J.Y. Lee, C.H. Park, C.S. Kim, Albumin-induced exfoliation of molybdenum disulfide nanosheets incorporated polycaprolactone/zein composite nanofibers for bone tissue regeneration, Mater. Sci. Eng. C. Mater. Biol. Appl. 116 (2020) 111162.

[39] S. Han, K. Han, J. Hong, D.Y. Yoon, C. Park, Y. Kim, Photothermal cellulose-patch with gold-spiked silica microrods based on Escherichia coli, ACS Omega 3 (5) (2018) 5244–5251.

[40] X.X. Yang, P. Feng, J. Cao, W. Liu, Y. Tang, Composition-engineered metal-organic framework-based microneedles for glucose-mediated transdermal insulin delivery, ACS Appl. Mater. Interfaces 12 (12) (2020) 13613–13621.

[41] Q. Sun, H. Bi, Z. Wang, C. Li, X. Wang, J. Xu, H. Zhu, R. Zhao, F. He, S. Gai, P. Yang, Hyaluronic acid-targeted and pH-responsive drug delivery system based on metal-organic frameworks for efficient antitumor therapy, Biomaterials 223 (2019) 119473.

[42] W. Shen, X. Chen, J. Luan, D. Wang, L. Yu, J. Ding, Sustained codelivery of cisplatin and paclitaxel via an injectable prodrug hydrogel for ovarian cancer treatment, ACS Appl. Mater. Interfaces 9 (46) (2017) 40031–40046.

[43] H. Liu, X. Shi, D. Wu, F. Kahsay Khshen, L. Deng, A. Dong, W. Wang, J. Zhang, Injectable, biodegradable, thermosensitive nanoparticles-aggregated hydrogel with tumor-specific targeting, penetration, and release for efficient postsurgical prevention of tumor recurrence, ACS Appl. Mater. Interfaces 11 (22) (2019) 19700–19711.

[44] M. Zhao, E. Bozzato, N. Joudiou, S. Ghiassinejad, F. Danhier, B. Gallez, V. Preat, Codelivery of paclitaxel and temozolomide through a photopolymerizable hydrogel prevents glioblastoma recurrence after surgical resection, J. Contr. Release 309 (2019) 72–81.

[45] Y. Liang, X. Zhao, T. Hu, Y. Han, B. Guo, Mussel-inspired, antibacterial, conductive, antioxidant, injectable composite hydrogel wound dressing to promote the regeneration of infected skin, J. Colloid Interface Sci. 556 (2019) 514–528.

[46] R. Samanipour, T. Wang, M. Werb, H. Hassannezhad, J.M.L. Rangel, M. Hoorfar, A. Hasan, C.K. Lee, S.R. Shin, Ferritin nanocage conjugated hybrid hydrogel for tissue engineering and drug delivery applications, ACS Biomater. Sci. Eng. 6 (1) (2020) 277–287.

[47] N. Alemdar, J. Leijten, G. Camci-Unal, J. Hjortnaes, J. Ribas, A. Paul, P. Mostafalu, A.K. Gaharwar, Y. Qiu, S. Sonkusale, R. Liao, A. Khademhosseini, Oxygen-generating photo-cross-linkable hydrogels support cardiac progenitor cell survival by reducing hypoxia-induced necrosis, ACS Biomater. Sci. Eng. 3 (9) (2017) 1964–1971.

[48] S.R. Shin, S.M. Jung, M. Zalabany, K. Kim, P. Zorlutuna, S.B. Kim, M. Nikkhah, M. Khabiry, M. Azize, J. Kong, K.T. Wan, T. Palacios, M.R. Dokmeci, H. Bae, X. S. Tang, A. Khademhosseini, Carbon-nanotube-embedded hydrogel sheets for engineering cardiac constructs and bioactuators, ACS Nano 7 (3) (2013) 2369–2380.

[49] M. Liu, H.J. Zhu, Y. Wang, C. Sevencan, B.L. Li, Functionalized MoS2-based nanomaterials for cancer phototherapy and other biomedical applications, ACS Mater. Lett. 3 (5) (2021) 462–496.

[50] H.J. Zhu, X.J. Loh, E.Y. Ye, Z.B. Li, Polymeric matrix-based nanoplatforms toward tumor therapy and diagnosis, ACS Mater. Lett. 4 (1) (2021) 21–48.

[51] X.L. Hu, H.J. Zhang, Z.J. Wang, C.Y.A. Shiu, Z. Gu, Microneedle array patches integrated with nanoparticles for therapy and diagnosis, Small 2 (4) (2021) 2000097.

[52] T.M. Tuan-Mahmood, M.T. McCrudden, B.M. Torrisi, E. McAlister, M.J. Garland, T.R. Singh, R.F. Donnelly, Microneedles for intradermal and transdermal drug delivery, Eur. J. Pharmaceut. Sci. 50 (5) (2013) 623–637.

[53] M.S. Gerstel, V.A. Place, Drug Delivery Device, Google Patents, 1976.

[54] S. Henry, D.V. McAllister, M.G. Allen, M.R. Prausnitz, Microfabricated microneedles: a novel approach to transdermal drug delivery, J. Pharmaceut. Sci. 87 (8) (1998) 922–925.

[55] G.G. Liversidge, P. Conzentino, Drug particle size reduction for decreasing gastric irritancy and enhancing absorption of naproxen in rats, Int. J. Pharm. 125 (2) (1995) 309–313.

[56] S.M. Pond, T.N. Tozer, First-pass elimination basic concepts and clinical consequences, Clin. Pharmacokinet. 9 (1) (1984) 1–25.

[57] A. Shahiwala, Formulation approaches in enhancement of patient compliance to oral drug therapy, Expet Opin. Drug Deliv. 8 (11) (2011) 1521–1529.

[58] P. Xue, X. Zhang, Y.J. Chuah, Y. Wu, Y. Kang, Flexible PEGDA-based microneedle patches with detachable PVP–CD arrowheads for transdermal drug delivery, RSC Adv. 5 (92) (2015) 75204–75209.

[59] S. Pradeep Narayanan, S. Raghavan, Fabrication and characterization of gold-coated solid silicon microneedles with improved biocompatibility, Int. J. Adv. Manuf. Technol. 104 (9–1) (2019) 3327–3333.

[60] T. Evens, O. Malek, S. Castagne, D. Seveno, A. Van Bael, A novel method for producing solid polymer microneedles using laser ablated moulds in an injection moulding process, Manufacture. Lett. 24 (2020) 29–32.

[61] Z. Hu, C.S. Meduri, R.S.J. Ingrole, H.S. Gill, G. Kumar, Solid and hollow metallic glass microneedles for transdermal drug-delivery, Appl. Phys. Lett. 116 (20) (2020) 203703.

[62] C. Yeung, S. Chen, B. King, H. Lin, K. King, F. Akhtar, G. Diaz, B. Wang, J. Zhu, W. Sun, A. Khademhosseini, S. Emaminejad, A 3D-printed microfluidic-enabled hollow microneedle architecture for transdermal drug delivery, Biomicrofluidics 13 (6) (2019), 064125.

[63] Y. Chen, B.Z. Chen, Q.L. Wang, X. Jin, X.D. Guo, Fabrication of coated polymer microneedles for transdermal drug delivery, J. Contr. Release 265 (2017) 14–21.

[64] S. Liang, Y. Zhang, H. Wang, Z. Xu, J. Chen, R. Bao, B. Tan, Y. Cui, G. Fan, W. Wang, W. Liu, Paintable and rapidly bondable conductive hydrogels as therapeutic cardiac patches, Adv. Mater. 30 (23) (2018), e1704235.

[65] Z. Zhou, X. Liu, W. Wu, S. Park, A.L. Miller Ii, A. Terzic, L. Lu, Effective nerve cell modulation by electrical stimulation of carbon nanotube embedded conductive polymeric scaffolds, Biomater. Sci. 6 (9) (2018) 2375–2385.

[66] C.E. Boone, C. Wang, M.A. Lopez-Ramirez, V. Beiss, S. Shukla, P.L. Chariou, D. Kupor, R. Rueda, J. Wang, N.F. Steinmetz, Active microneedle administration of plant virus nanoparticles for cancer in situ vaccination improves immunotherapeutic efficacy, ACS Appl. Nano Mater. 3 (8) (2020) 8037–8051.

[67] H.W. Yang, L. Ye, X.D. Guo, C. Yang, R.W. Compans, M.R. Prausnitz, Ebola vaccination using a DNA vaccine coated on PLGA-PLL/gammaPGA nanoparticles administered using a microneedle patch, Adv. Health Mater. 6 (1) (2017) 1600750.

[68] S.P. Sullivan, D.G. Koutsonanos, M. Del Pilar Martin, J.W. Lee, V. Zarnitsyn, S. O. Choi, N. Murthy, R.W. Compans, I. Skountzou, M.R. Prausnitz, Dissolving polymer microneedle patches for influenza vaccination, Nat. Med. 16 (8) (2010) 915–920.

[69] J. Kennedy, E. Larraneta, M.T.C. McCrudden, C.M. McCrudden, A.J. Brady, S. J. Fallows, H.O. McCarthy, A. Kissenpfennig, R.F. Donnelly, In vivo studies investigating biodistribution of nanoparticle-encapsulated rhodamine B delivered via dissolving microneedles, J. Contr. Release 265 (2017) 57–65.

[70] C.J. Ke, Y.J. Lin, Y.C. Hu, W.L. Chiang, K.J. Chen, W.C. Yang, H.L. Liu, C.C. Fu, H. W. Sung, Multidrug release based on microneedle arrays filled with pH-responsive PLGA hollow microspheres, Biomaterials 33 (20) (2012) 5156–5165.

[71] M.A. Lopez-Ramirez, F. Soto, C. Wang, R. Rueda, S. Shukla, C. Silva-Lopez, D. Kupor, D.A. McBride, J.K. Pokorski, A. Nourhani, N.F. Steinmetz, N.J. Shah, J. Wang, Built-in active microneedle patch with enhanced autonomous drug delivery, Adv. Mater. 32 (1) (2020), e1905740.

[72] K. Ahmed Saeed Al-Japairai, S. Mahmood, S. Hamed Almurisi, J. Reddy Venugopal, A. Rebhi Hilles, M. Azmana, S. Raman, Current trends in polymer microneedle for transdermal drug delivery, Int. J. Pharm. 587 (2020) 119673.

[73] R. He, Y. Niu, Z. Li, A. Li, H. Yang, F. Xu, F. Li, A hydrogel microneedle patch for point-of-care testing based on skin interstitial fluid, Adv. Healthcare Mater. 9 (4) (2020), e1901201.

[74] E. McAlister, B. Dutton, L.K. Vora, L. Zhao, A. Ripolin, D. Zahari, H.L. Quinn, I. A. Tekko, A.J. Courtenay, S.A. Kelly, A.M. Rodgers, L. Steiner, G. Levin, E. Levy-Nissenbaum, N. Shterman, H.O. McCarthy, R.F. Donnelly, Directly compressed tablets: a novel drug-containing reservoir combined with hydrogel-forming microneedle arrays for transdermal drug delivery, Adv. Healthcare Mater. 10 (3) (2021), e2001256.

[75] X. Hu, J. Yu, C. Qian, Y. Lu, A.R. Kahkoska, Z. Xie, X. Jing, J.B. Buse, Z. Gu, H$_2$O$_2$-Responsive vesicles integrated with transcutaneous patches for glucose-mediated insulin delivery, ACS Nano 11 (1) (2017) 613–620.

[76] D. Shen, H. Yu, L. Wang, X. Chen, J. Feng, C. Li, W. Xiong, Q. Zhang, Glucose-responsive hydrogel-based microneedles containing phenylborate ester bonds and N-isopropylacrylamide moieties and their transdermal drug delivery properties, Eur. Polym. J. 148 (2021) 110348.

[77] G. Yang, Q. Chen, D. Wen, Z. Chen, J. Wang, G. Chen, Z. Wang, X. Zhang, Y. Zhang, Q. Hu, L. Zhang, Z. Gu, A therapeutic microneedle patch made from hair-derived keratin for promoting hair regrowth, ACS Nano 13 (4) (2019) 4354–4360.

[78] E.M. Ahmed, Hydrogel: preparation, characterization, and applications: a review, J. Adv. Res. 6 (2) (2015) 105–121.

[79] G. Barouti, S.S. Liow, Q. Dou, H. Ye, C. Orione, S.M. Guillaume, X.J. Loh, New linear and star-shaped thermogelling poly ([R]-3-hydroxybutyrate) copolymers, Chem. Euro. J. 22 (30) (2016) 10501–10512.

[80] L. Gan, G.R. Deen, X. Loh, Y. Gan, New stimuli-responsive copolymers of N-acryloyl-N′-alkyl piperazine and methyl methacrylate and their hydrogels, Polymer 42 (1) (2001) 65–69.

[81] L. Jiang, Z. Luo, X.J. Loh, Y.L. Wu, Z.B. Li, PHA-based thermogel as a controlled zero-order chemotherapeutic delivery system for the effective treatment of melanoma, Acs Appl. BioMater. 2 (8) (2019) 3591–3600.

[82] Q.Y. Lin, J.Y.C. Lim, K. Xue, X.Y. Su, X.J. Loh, Polymeric hydrogels as a vitreous replacement strategy in the eye, Biomaterials 268 (2021) 120547.

[83] X.J. Loh, V.P.N. Nguyen, N. Kuo, J. Li, Encapsulation of basic fibroblast growth factor in thermogelling copolymers preserves its bioactivity, J. Mater. Chem. 21 (7) (2011) 2246–2254.

[84] V.P.N. Nguyen, N. Kuo, X.J. Loh, New biocompatible thermogelling copolymers containing ethylene-butylene segments exhibiting very low gelation concentrations, Soft Matter 7 (5) (2011) 2150–2159.

[85] E. Caló, V.V. Khutoryanskiy, Biomedical applications of hydrogels: a review of patents and commercial products, Eur. Polym. J. 65 (2015) 252–267.

[86] M.F. Refojo, Permeation of water through some hydrogels, J. Appl. Polym. Sci. 9 (10) (1965) 3417–3426.

[87] M. Barvicč, K. Kliment, M. Zavadil, Biologic properties and possible uses of polymer-like sponges, J. Biomed. Mater. Res. 1 (3) (1967) 313–323.

[88] J. Drobník, P. Špaček, O. Wichterle, Diffusion of anti-tumor drugs through membranes from hydrophilic methacrylate gels, J. Biomed. Mater. Res. 8 (1) (1974) 45–51.

[89] X. Liu, W.S. Heng, Paul, Q. Li, L.W. Chan, Novel polymeric microspheres containing norcantharidin for chemoembolization, J. Contr. Release 116 (1) (2006) 35–41.

[90] K.H. Bouhadir, E. Alsberg, D.J. Mooney, Hydrogels for combination delivery of antineoplastic agents, Biomaterials 22 (19) (2001) 2625–2633.

[91] J.R. McDaniel, D.J. Callahan, A. Chilkoti, Drug delivery to solid tumors by elastin-like polypeptides, Adv. Drug Deliv. Rev. 62 (15) (2010) 1456–1467.

[92] L.P. Rivory, E. Chatelut, P. Canal, A. Mathieu-Boue, J. Robert, Kinetics of the in vivo interconversion of the carboxylate and lactone forms of irinotecan (CPT-11) and of its metabolite SN-38 in patients, Cancer Res. 54 (24) (1994) 6330–6333.

[93] J. Wang, F. Tang, Y. Wang, Q. Lu, S. Liu, L. Li, Self-healing and highly stretchable gelatin hydrogel for self-powered strain sensor, ACS Appl. Mater. Interfaces 12 (1) (2020) 1558–1566.

[94] X. Liu, Y. Yang, Y. Li, X. Niu, B. Zhao, Y. Wang, C. Bao, Z. Xie, Q. Lin, L. Zhu, Integration of stem cell-derived exosomes with in situ hydrogel glue as a promising tissue patch for articular cartilage regeneration, Nanoscale 9 (13) (2017) 4430–4438.

[95] H.J. Won, B. Ryplida, S.G. Kim, G. Lee, J.H. Ryu, S.Y. Park, Diselenide-bridged carbon-dot-mediated self-healing, conductive, and adhesive wireless hydrogel sensors for label-free breast cancer detection, ACS Nano 14 (7) (2020) 8409–8420.

[96] N. Arabi, A. Zamanian, Effect of cooling rate and gelatin concentration on the microstructural and mechanical properties of ice template gelatin scaffolds, Biotechnol. Appl. Biochem. 60 (6) (2013) 573–579.

[97] T. Wu, C. Cui, Y. Huang, Y. Liu, C. Fan, X. Han, Y. Yang, Z. Xu, B. Liu, G. Fan, W. Liu, Coadministration of an adhesive conductive hydrogel patch and an injectable hydrogel to treat myocardial infarction, ACS Appl. Mater. Interfaces 12 (2) (2020) 2039–2048.

[98] X. Zhao, Q. Lang, L. Yildirimer, Z.Y. Lin, W. Cui, N. Annabi, K.W. Ng, M. R. Dokmeci, A.M. Ghaemmaghami, A. Khademhosseini, Photocrosslinkable gelatin hydrogel for epidermal tissue engineering, Adv. Healthcare Mater. 5 (1) (2016) 108–118.

[99] J.W. Nichol, S.T. Koshy, H. Bae, C.M. Hwang, S. Yamanlar, A. Khademhosseini, Cell-laden microengineered gelatin methacrylate hydrogels, Biomaterials 31 (21) (2010) 5536–5544.

[100] C. Xu, Y. Xu, M. Yang, Y. Chang, A. Nie, Z. Liu, J. Wang, Z. Luo, Black-phosphorus-incorporated hydrogel as a conductive and biodegradable platform for enhancement of the neural differentiation of mesenchymal stem cells, Adv. Funct. Mater. 30 (39) (2020) 2000177.

[101] K.J. Wolf, S. Kumar, Hyaluronic acid: incorporating the bio into the material, ACS Biomater. Sci. Eng. 5 (8) (2019) 3753–3765.

[102] G. Huang, H. Huang, Hyaluronic acid-based biopharmaceutical delivery and tumor-targeted drug delivery system, J. Contr. Release 278 (2018) 122–126.

[103] Z. Luo, Y. Dai, H. Gao, Development and application of hyaluronic acid in tumor targeting drug delivery, Acta Pharm. Sin. B 9 (6) (2019) 1099–1112.

[104] J. Shin, E.J. Choi, J.H. Cho, A.N. Cho, Y. Jin, K. Yang, C. Song, S.W. Cho, Three-dimensional electroconductive hyaluronic acid hydrogels incorporated with carbon nanotubes and polypyrrole by catechol-mediated dispersion enhance neurogenesis of human neural stem cells, Biomacromolecules 18 (10) (2017) 3060–3072.

[105] C. Antich, J. de Vicente, G. Jimenez, C. Chocarro, E. Carrillo, E. Montanez, P. Galvez-Martin, J.A. Marchal, Bio-inspired hydrogel composed of hyaluronic acid and alginate as a potential bioink for 3D bioprinting of articular cartilage engineering constructs, Acta Biomater. 106 (2020) 114–123.

[106] J. Shin, S. Choi, J.H. Kim, J.H. Cho, Y. Jin, S. Kim, S. Min, S.K. Kim, D. Choi, S. W. Cho, Tissue Tapes—phenolic hyaluronic acid hydrogel patches for off-the-shelf therapy, Adv. Funct. Mater. 29 (49) (2019) 1903863.

[107] J.B. Wolinsky, Y.L. Colson, M.W. Grinstaff, Local drug delivery strategies for cancer treatment: gels, nanoparticles, polymeric films, rods, and wafers, J. Contr. Release 159 (1) (2012) 14–26.

[108] M.A. Moses, H. Brem, R. Langer, Advancing the field of drug delivery: taking aim at cancer, Cancer Cell 4 (5) (2003) 337–341.

[109] R. Langer, Implantable controlled release systems, Pharmacol. Ther. 21 (1) (1983) 35–51.

[110] A.S. Hoffman, The origins and evolution of "controlled" drug delivery systems, J. Contr. Release 132 (3) (2008) 153–163.

[111] M. Milovanovic, A. Arsenijevic, J. Milovanovic, T. Kanjevac, N. Arsenijevic, in: A. M. Grumezescu (Ed.), Chapter 14 - Nanoparticles in Antiviral Therapy, Antimicrobial Nanoarchitectonics, Elsevier, 2017, pp. 383–410.

[112] W. Liu, B.S. Lee, W.F. Mieler, J.J. Kang-Mieler, Biodegradable microsphere-hydrogel ocular drug delivery system for controlled and extended release of bioactive aflibercept in vitro, Curr. Eye Res. 44 (3) (2019) 264–274.

[113] L. Fan, M. Duan, X. Sun, H. Wang, J. Liu, Injectable liquid metal- and methotrexate-loaded microsphere for cancer chemophotothermal synergistic therapy, ACS Appl. BioMater. 3 (6) (2020) 3553–3559.

[114] M.Y. Hsu, Y.T. Huang, C.J. Weng, C.M. Chen, Y.F. Su, S.Y. Chu, J.H. Tseng, R. C. Wu, S.J. Liu, Preparation and in vitro/in vivo evaluation of doxorubicin-loaded poly[lactic-co-glycol acid] microspheres using electrospray method for sustained drug delivery and potential intratumoral injection, Colloids Surf. B Biointerfaces 190 (2020) 110937.

[115] R. Sobel, R. Versic, A.G. Gaonkar, Introduction to microencapsulation and controlled delivery in foods, Microencapsul. Food. Industry., pp. 3-12..

[116] J. Jia, C. Wang, K. Chen, Y. Yin, Drug release of yolk/shell microcapsule controlled by pH-responsive yolk swelling, Chem. Eng. J. 327 (2017) 953–961.

[117] Y. Chen, W. Wei, Y. Zhu, J. Luo, R. Liu, X. Liu, Synthesis of temperature/pH dual-stimuli-response multicompartmental microcapsules via pickering emulsion for preprogrammable payload release, ACS Appl. Mater. Interfaces 12 (4) (2020) 4821–4832.

[118] J.W. Kim, S.S. Lee, J. Park, M. Ku, J. Yang, S.H. Kim, Smart microcapsules with molecular polarity- and temperature-dependent permeability, Small 15 (21) (2019), e1900434.

[119] Y. Kamiya, Y. Yamada, T. Muro, K. Matsuura, H. Asanuma, DNA microcapsule for photo-triggered drug release systems, ChemMedChem 12 (24) (2017) 2016–2021.

[120] H. Bi, X. Han, Magnetic field triggered drug release from lipid microcapsule containing lipid-coated magnetic nanoparticles, Chem. Phys. Lett. 706 (2018) 455–460.

[121] B. Mohanraj, G. Duan, A. Peredo, M. Kim, F. Tu, D. Lee, G.R. Dodge, R.L. Mauck, Mechanically-activated microcapsules for 'on-demand' drug delivery in dynamically loaded musculoskeletal tissues, Adv. Funct. Mater. 29 (15) (2019) 1807909.

[122] A. Nicolae, A.M. Grumezescu, Chapter 1 - polymer fibers in biomedical engineering, in: V. Grumezescu, A.M. Grumezescu (Eds.), Materials for Biomedical Engineering, Elsevier, 2019, pp. 1–20.

[123] Y. Yang, D. Lei, S. Huang, Q. Yang, B. Song, Y. Guo, A. Shen, Z. Yuan, S. Li, F. L. Qing, X. Ye, Z. You, Q. Zhao, Elastic 3D-printed hybrid polymeric scaffold improves cardiac remodeling after myocardial infarction, Adv. Healthcare Mater. 8 (10) (2019), e1900065.

[124] B. Maharjan, V.K. Kaliannagounder, S.R. Jang, G.P. Awasthi, D.P. Bhattarai, G. Choukrani, C.H. Park, C.S. Kim, In-situ polymerized polypyrrole nanoparticles immobilized poly(epsilon-caprolactone) electrospun conductive scaffolds for bone tissue engineering, Mater. Sci. Eng. C Mater. Biol. Appl. 114 (2020) 111056.

[125] M.N. Sithole, P. Kumar, L.C. du Toit, T. Marimuthu, Y.E. Choonara, V. Pillay, A 3D bioprinted in situ conjugated-co-fabricated scaffold for potential bone tissue engineering applications, J. Biomed. Mater. Res. 106 (5) (2018) 1311–1321.

[126] F. Ghorbani, A. Zamanian, An efficient functionalization of dexamethasone-loaded polymeric scaffold with [3-(2,3-epoxypropoxy)-propyl]-trimethoxysilane coupling agent for bone regeneration: synthesis, characterization, and in vitro evaluation, J. Bioact. Compat Polym. 35 (2) (2020) 139–159.

[127] S. Babitha, P.S. Korrapati, Biodegradable zein-polydopamine polymeric scaffold impregnated with TiO_2 nanoparticles for skin tissue engineering, Biomed. Mater. 12 (5) (2017), 055008.

[128] H. Zigdon-Giladi, A. Khutaba, R. Elimelech, E.E. Machtei, S. Srouji, VEGF release from a polymeric nanofiber scaffold for improved angiogenesis, J. Biomed. Mater. Res. 105 (10) (2017) 2712–2721.

[129] C.M. Andres, I. Larraza, T. Corrales, N.A. Kotov, Nanocomposite microcontainers, Adv. Mater. 24 (34) (2012) 4597–4600.

[130] M.V. Kiryukhin, S.M. Man, A. Tonoyan, H.Y. Low, G.B. Sukhorukov, Adhesion of polyelectrolyte multilayers: sealing and transfer of microchamber arrays, Langmuir 28 (13) (2012) 5678–5686.

[131] M. Gai, M.A. Kurochkin, D. Li, B.N. Khlebtsov, L. Dong, N. Tarakina, R. Poston, D. J. Gould, J. Frueh, G.B. Sukhorukov, In-situ NIR-laser mediated bioactive substance delivery to single cell for EGFP expression based on biocompatible microchamber-arrays, J. Contr. Release 276 (2018) 84–92.

[132] O. Kopach, K. Zheng, O.A. Sindeeva, M. Gai, G.B. Sukhorukov, D.A. Rusakov, Polymer microchamber arrays for geometry-controlled drug release: a functional study in human cells of neuronal phenotype, Biomater. Sci. 7 (6) (2019) 2358–2371.

[133] Y. Zykova, V. Kudryavtseva, M. Gai, A. Kozelskaya, J. Frueh, G. Sukhorukov, S. Tverdokhlebov, Free-standing microchamber arrays as a biodegradable drug depot system for implant coatings, Eur. Polym. J. 114 (2019) 72–80.

[134] J. Zhang, R. Sun, A.O. DeSouza-Edwards, J. Frueh, G.B. Sukhorukov, Microchamber arrays made of biodegradable polymers for enzymatic release of small hydrophilic cargos, Soft Matter 16 (9) (2020) 2266–2275.

[135] H. zur Hausen, Papillomaviruses and cancer: from basic studies to clinical application, Nat. Rev. Cancer 2 (5) (2002) 342–350.

[136] F. Dimitriou, R. Krattinger, E. Ramelyte, M.J. Barysch, S. Micaletto, R. Dummer, S.M. Goldinger, The world of melanoma: epidemiologic, genetic, and anatomic differences of melanoma across the globe, Curr. Oncol. Rep. 20 (11) (2018) 87.

[137] M. Stumvoll, B.J. Goldstein, T.W. van Haeften, Type 2 diabetes: principles of pathogenesis and therapy, Lancet 365 (9467) (2005) 1333–1346.

[138] J.M. Bumpous, J.T. Johnson, The infected wound and its management, Otolaryngol. Clin. 28 (5) (1995) 987–1001.

[139] T. Pap, A. Korb-Pap, Cartilage damage in osteoarthritis and rheumatoid arthritis–two unequal siblings, Nat. Rev. Rheumatol. 11 (10) (2015) 606–615.

[140] V.F. Segers, R.T. Lee, Stem-cell therapy for cardiac disease, Nature 451 (7181) (2008) 937–942.

[141] P.G. Kopelman, Obesity as a medical problem, Nature 404 (6778) (2000) 635–643.

[142] N. Vlassova, A. Han, J.M. Zenilman, G. James, G.S. Lazarus, New horizons for cutaneous microbiology: the role of biofilms in dermatological disease, Br. J. Dermatol. 165 (4) (2011) 751–759.

[143] J. Yu, Y. Zhang, Y. Ye, R. DiSanto, W. Sun, D. Ranson, F.S. Ligler, J.B. Buse, Z. Gu, Microneedle-array patches loaded with hypoxia-sensitive vesicles provide fast glucose-responsive insulin delivery, Proc. Natl. Acad. Sci. U. S. A. 112 (27) (2015) 8260–8265.

[144] Y. Ye, J. Yu, C. Wang, N.Y. Nguyen, G.M. Walker, J.B. Buse, Z. Gu, Microneedles integrated with pancreatic cells and synthetic glucose-signal amplifiers for smart insulin delivery, Adv. Mater. 28 (16) (2016) 3115–3121.

[145] J. Yu, C. Qian, Y. Zhang, Z. Cui, Y. Zhu, Q. Shen, F.S. Ligler, J.B. Buse, Z. Gu, Hypoxia and H_2O_2 dual-sensitive vesicles for enhanced glucose-responsive insulin delivery, Nano Lett. 17 (2) (2017) 733–739.

[146] G.H. Jiang, B. Xu, J.Y. Zhu, Y. Zhang, T.Q. Liu, G. Song, Polymer microneedles integrated with glucose-responsive mesoporous bioactive glass nanoparticles for transdermal delivery of insulin, Biomed. Phys. Eng. Express. 5 (6) (2019), 045038.

[147] Y.H. Lin, W. Hu, X.W. Bai, Y.S. Ju, C. Cao, S.F. Zou, Z.Z. Tong, C. Cen, G.H. Jiang, X.D. Kong, Glucose- and pH-responsive supramolecular polymer vesicles based on Host−Guest interaction for transcutaneous delivery of insulin, ACS Appl. BioMater. 3 (4) (2020) 6376–6383.

[148] W. Chen, R. Tian, C. Xu, B.C. Yung, G. Wang, Y. Liu, Q. Ni, F. Zhang, Z. Zhou, J. Wang, G. Niu, Y. Ma, L. Fu, X. Chen, Microneedle-array patches loaded with dual mineralized protein/peptide particles for type 2 diabetes therapy, Nat. Commun. 8 (1) (2017) 1777.

[149] B. Xu, Q. Cao, Y. Zhang, W. Yu, J. Zhu, D. Liu, G. Jiang, Microneedles integrated with ZnO quantum-dot-capped mesoporous bioactive glasses for glucose-mediated insulin delivery, ACS Biomater. Sci. Eng. 4 (7) (2018) 2473–2483.

[150] D. Liu, B. Yu, G. Jiang, W. Yu, Y. Zhang, B. Xu, Fabrication of composite microneedles integrated with insulin-loaded CaCO_3 microparticles and PVP for transdermal delivery in diabetic rats, Mater. Sci. Eng. C. Mater. Biol. Appl. 90 (2018) 180–188.

[151] Z. Wang, H. Li, J. Wang, Z. Chen, G. Chen, D. Wen, A. Chan, Z. Gu, Transdermal colorimetric patch for hyperglycemia sensing in diabetic mice, Biomaterials 237 (2020) 119782.

[152] Z. Tong, J. Zhou, J. Zhong, Q. Tang, Z. Lei, H. Luo, P. Ma, X. Liu, Glucose- and H_2O_2-responsive polymeric vesicles integrated with microneedle patches for glucose-sensitive transcutaneous delivery of insulin in diabetic rats, ACS Appl. Mater. Interfaces 10 (23) (2018) 20014–20024.

[153] B. Xu, G. Jiang, W. Yu, D. Liu, Y. Zhang, J. Zhou, S. Sun, Y. Liu, H_2O_2-Responsive mesoporous silica nanoparticles integrated with microneedle patches for the glucose-monitored transdermal delivery of insulin, J. Mater. Chem. B 5 (41) (2017) 8200–8208.

[154] Y. Zhang, J. Wang, J. Yu, D. Wen, A.R. Kahkoska, Y. Lu, X. Zhang, J.B. Buse, Z. Gu, Bioresponsive microneedles with a sheath structure for H_2O_2 and pH cascade-triggered insulin delivery, Small 14 (14) (2018), e1704181.

[155] Y.J. Zhang, J.W. Li, M.X. Wu, Z.Y. Guo, D. Guo, X.H. Zhou, Y.P. Li, S. Liu, L.J. Xue, Y.F. Lei, Glucose-responsive gold nanocluster-loaded microneedle patch for type 1 diabetes therapy, ACS Appl. BioMater. 3 (9) (2020) 8640–8649.

[156] Y.P. Wang, S.Y. Cheng, W. Hu, X. Xue Lin, C. Cao, S.F. Zou, Z.Z. Tong, G.H. Jiang, X.D. Kong, Polymer-grafted hollow mesoporous silica nanoparticles integrated with microneedle patches for glucose-responsive drug delivery, Front. Mater. Sci. 15 (1) (2021) 98–112.

[157] W. Yu, G. Jiang, Y. Zhang, D. Liu, B. Xu, J. Zhou, Near-infrared light triggered and separable microneedles for transdermal delivery of metformin in diabetic rats, J. Mater. Chem. B 5 (48) (2017) 9507–9513.

[158] Y. Zhang, D. Wang, M. Gao, B. Xu, J. Zhu, W. Yu, D. Liu, G. Jiang, Separable microneedles for near-infrared light-triggered transdermal delivery of metformin in diabetic rats, ACS Biomater. Sci. Eng. 4 (8) (2018) 2879–2888.

[159] Y. Zhang, J.H. Jiang, W.J. Hong, M.Y. Gao, B. Xu, J.Y. Zhu, G. Song, T.Q. Liu, Polymeric microneedles integrated with metformin-loaded and PDA/LA-Coated hollow mesoporous SiO_2 for NIR-triggered transdermal delivery on diabetic rats, ACS Appl. BioMater. 1 (6) (2018) 1906–1917.

[160] J. Di, J.C. Yu, Q. Wang, S.S. Yao, D.J. Suo, Y.Q. Ye, M. Pless, Y. Zhu, Y. Jing, Z. Gu, Ultrasound-triggered noninvasive regulation of blood glucose levels using microgels integrated with insulin nanocapsules, Nano Res. 10 (4) (2017) 1393–1402.

[161] A. Ahsana, M.A. Farooq, Therapeutic potential of green synthesized silver nanoparticles loaded PVA hydrogel patches for wound healing, J. Drug Deliv. Sci. Technol. 54 (2019) 101308.

[162] S.E. Kim, A.P. Tiwari, Mussel-inspired polydopamine-enabled in situ-synthesized silver nanoparticleanchored porous polyacrylonitrile nanofibers for wound-healing applications, Int. J. Polymer. Mater. Polymer. Biomater. 8 (1) (2020) 471–480.

[163] H. Haidari, Z. Kopecki, A.T. Sutton, S. Garg, A.J. Cowin, K. Vasilev, pH-responsive "smart" hydrogel for controlled delivery of silver nanoparticles to infected wounds, Antibiotics 10 (1) (2021) 49.

[164] J.J. Zhu, G.H. Jiang, G. Song, T.Q. Liu, C. Cao, Y.H. Yang, Y.J. Zhang, W.J. Hong, Incorporation of ZnO/bioactive glass nanoparticles into alginate/chitosan composite hydrogels for wound closure, ACS Appl. BioMater. 2 (9) (2019) 5042–5052.

[165] C. Mao, Y. Xiang, X. Liu, Z. Cui, X. Yang, K.W.K. Yeung, H. Pan, X. Wang, P. K. Chu, S. Wu, Photo-inspired antibacterial activity and wound healing acceleration by hydrogel embedded with Ag/Ag@AgCl/ZnO nanostructures, ACS Nano 11 (9) (2017) 9010–9021.

[166] Q.Z. Xu, Y.Y. Wang, T.J. Chen, C.W. Lao, H.K. Gao, R. Wei, B. Feng, W. Zhi, J. Weng, J.X. Wang, A distinctive nanocomposite hydrogel integrated platform for the healing of wound after the resection of melanoma, Materialia. 14 (2020) 100931.

[167] J. Qu, X. Zhao, Y. Liang, T. Zhang, P.X. Ma, B. Guo, Antibacterial adhesive injectable hydrogels with rapid self-healing, extensibility and compressibility as wound dressing for joints skin wound healing, Biomaterials 183 (2018) 185–199.

[168] K. Fang, R. Wang, H. Zhang, L. Zhou, T. Xu, Y. Xiao, Y. Zhou, G. Gao, J. Chen, D. Liu, F. Ai, J. Fu, Mechano-responsive, tough, and antibacterial zwitterionic hydrogels with controllable drug release for wound healing applications, ACS Appl. Mater. Interfaces 12 (47) (2020) 52307–52318.

[169] X. Gong, C. Hou, Q. Zhang, Y. Li, H. Wang, Thermochromic hydrogel-functionalized textiles for synchronous visual monitoring of on-demand in vitro drug release, ACS Appl. Mater. Interfaces 12 (46) (2020) 51225–51235.

[170] A. Gupta, S.M. Briffa, S. Swingler, H. Gibson, V. Kannappan, G. Adamus, M. Kowalczuk, C. Martin, I. Radecka, Synthesis of silver nanoparticles using curcumin-cyclodextrins loaded into bacterial cellulose-based hydrogels for wound dressing applications, Biomacromolecules 21 (5) (2020) 1802–1811.

[171] B. Tao, C. Lin, Y. Deng, Z. Yuan, X. Shen, M. Chen, Y. He, Z. Peng, Y. Hu, K. Cai, Copper-nanoparticle-embedded hydrogel for killing bacteria and promoting wound healing with photothermal therapy, J. Mater. Chem. B 7 (15) (2019) 2534–2548.

[172] H. Ma, Q. Zhou, J. Chang, C. Wu, Grape seed-inspired smart hydrogel scaffolds for melanoma therapy and wound healing, ACS Nano 13 (4) (2019) 4302–4311.

[173] W. Yan, X. Xu, Q. Xu, Z. Sun, Z. Lv, R. Wu, Q. Jiang, D. Shi, An injectable hydrogel scaffold with kartogenin-encapsulated nanoparticles for porcine cartilage regeneration: a 12-month follow-up study, Am. J. Sports Med. 48 (13) (2020) 3233–3244.

[174] B. Mohanraj, G. Duan, A. Peredo, M. Kim, F. Tu, D. Lee, G.R. Dodge, R.L. Mauck, Mechanically-activated microcapsules for 'on-demand' drug delivery in dynamically loaded musculoskeletal tissues, Adv. Funct. Mater. 29 (15) (2019) 1807909.

[175] H. Yu, H. Zhao, C. Huang, Y. Du, Mechanically and electrically enhanced CNT-collagen hydrogels as potential scaffolds for engineered cardiac constructs, ACS Biomater. Sci. Eng. 3 (11) (2017) 3017–3021.

[176] Z. Zhang, P.C. Tsai, T. Ramezanli, B.B. Michniak-Kohn, Polymeric nanoparticles-based topical delivery systems for the treatment of dermatological diseases, Wilry. Interdiscip. Rev. Nanomed. Nanobiotechnol. 5 (3) (2013) 205–218.

[177] E. Hahnel, U. Blume-Peytavi, C. Trojahn, G. Dobos, I. Jahnke, V. Kanti, C. Richter, A. Lichterfeld-Kottner, N. Garcia Bartels, J. Kottner, Prevalence and associated factors of skin diseases in aged nursing home residents: a multicentre prevalence study, BMJ Open 7 (9) (2017), e018283.

[178] C.W.X. Tan, W.D. Tan, R. Srivastava, A.P. Yow, D.W.K. Wong, H.L. Tey, Dissolving triamcinolone-embedded microneedles for the treatment of keloids: a single-blinded intra-individual controlled clinical trial, Dermatol. Ther. 9 (3) (2019) 601–611.

[179] D.C. Yeo, E.R. Balmayor, J.T. Schantz, C. Xu, Microneedle physical contact as a therapeutic for abnormal scars, Eur. J. Med. Res. 22 (1) (2017) 28.

[180] S. Mukherjee, A. Date, V. Patravale, H.C. Korting, A. Roeder, G. Weindl, Retinoids in the treatment of skin aging: an overview of clinical efficacy and safety, Clin. Interv. Aging 1 (4) (2006) 327–348.

[181] B. Limcharoen, P. Toprangkobsin, M. Kroger, M.E. Darvin, T. Sansureerungsikul, T. Rujiwaree, S. Wanichwecharungruang, W. Banlunara, J. Lademann, A. Patzelt, Microneedle-facilitated intradermal proretinal nanoparticle delivery, Nanomaterials 10 (2) (2020) 368.

[182] Y. Xie, H. Wang, J. Mao, Y. Li, M. Hussain, J. Zhu, L. Zhang, J. Tao, Enhanced in vitro efficacy for inhibiting hypertrophic scar by bleomycin-loaded dissolving hyaluronic acid microneedles, J. Mater. Chem. B 7 (42) (2019) 6604–6611.

[183] S. Lin, G. Quan, A. Hou, P. Yang, T. Peng, Y. Gu, W. Qin, R. Liu, X. Ma, X. Pan, H. Liu, L. Wang, C. Wu, Strategy for hypertrophic scar therapy: improved delivery of triamcinolone acetonide using mechanically robust tip-concentrated dissolving microneedle array, J. Contr. Release 306 (2019) 69–82.

[184] M. Wang, Y. Han, X. Yu, L. Liang, H. Chang, D.C. Yeo, C. Wiraja, M.L. Wee, L. Liu, X. Liu, C. Xu, Upconversion nanoparticle powered microneedle patches for transdermal delivery of siRNA, Adv. Health Mater. 9 (2) (2020), e1900635.

[185] Y. Zhang, P. Feng, J. Yu, J. Yang, J. Zhao, J. Wang, Q. Shen, Z. Gu, ROS-responsive microneedle patch for acne vulgaris treatment, Adv. Ther. 1 (2017) 1800035.

[186] Y. Zhang, Q. Liu, J. Yu, S. Yu, J. Wang, L. Qiang, Z. Gu, Locally induced adipose tissue browning by microneedle patch for obesity treatment, ACS Nano 11 (9) (2017) 9223–9230.

[187] S. Fakhraei Lahiji, S.H. Seo, S. Kim, M. Dangol, J. Shim, C.G. Li, Y. Ma, C. Lee, G. Kang, H. Yang, K.Y. Choi, H. Jung, Transcutaneous implantation of valproic acid-encapsulated dissolving microneedles induces hair regrowth, Biomaterials 167 (2018) 69–79.

[188] P. Zan, A. Than, W. Zhang, H.X. Cai, W. Zhao, P. Chen, Transdermal photothermal-pharmacotherapy to remodel adipose tissue for obesity and metabolic disorders, ACS Nano 16 (2) (2022) 1813–1825.

[189] I.J. Choi, A. Kang, M.H. Ahn, H. Jun, S.K. Baek, J.H. Park, W. Na, S.O. Choi, Insertion-responsive microneedles for rapid intradermal delivery of canine influenza vaccine, J. Contr. Release 286 (2018) 460–466.

[190] G. Du, R.M. Hathout, M. Nasr, M.R. Nejadnik, J. Tu, R.I. Koning, A.J. Koster, B. Slutter, A. Kros, W. Jiskoot, J.A. Bouwstra, J. Monkare, Intradermal vaccination with hollow microneedles: a comparative study of various protein antigen and adjuvant encapsulated nanoparticles, J. Contr. Release 266 (2017) 109–118.

[191] J.F. Liao, J.C. Lee, C.K. Lin, K.C. Wei, P.Y. Chen, H.W. Yang, Self-assembly DNA polyplex vaccine inside dissolving microneedles for high-potency intradermal vaccination, Theranostics 7 (10) (2017) 2593–2605.

[192] A.A. Ali, C.M. McCrudden, J. McCaffrey, J.W. McBride, G. Cole, N.J. Dunne, T. Robson, A. Kissenpfennig, R.F. Donnelly, H.O. McCarthy, DNA vaccination for cervical cancer; a novel technology platform of RALA mediated gene delivery via polymeric microneedles, Nanomedicine 13 (3) (2017) 921–932.

[193] H.T.T. Duong, Y. Yin, T. Thambi, B.S. Kim, J.H. Jeong, D.S. Lee, Highly potent intradermal vaccination by an array of dissolving microneedle polypeptide cocktails for cancer immunotherapy, J. Mater. Chem. B 8 (6) (2020) 1171–1181.